Solar Magnetoconvection and Small-Scale Dynamo

Recent Developments in Observation and Simulation

J.M. Borrero[1] · **S. Jafarzadeh**[2] · **M. Schüssler**[3] ·
S.K. Solanki[3,4]

Abstract A number of observational and theoretical aspects of solar magnetoconvection are considered in this review. We discuss recent developments in our understanding of the small-scale structure of the magnetic field on the solar surface and its interaction with convective flows, which is at the centre of current research. Topics range from plage areas in active regions over the magnetic network shaped by supergranulation to the ubiquituous 'turbulent' internetwork fields. On the theoretical side, we focus upon magnetic field generation by small-scale dynamo action.

1 Introduction

New observational facilities and instruments (on the ground and in space), innovative methods for data analysis, and the rapid growth of computing power have led to considerable progress in our understanding of solar magnetoconvective processes during the last decade. This ranges all the way from the smallest observable magnetic structures in 'quiet' areas to the dynamical fine structure of sunspot umbrae and penumbrae. The interplay of observations and radiative 3D-MHD simulations is crucial for this progress: simulations permit us to identify the physical processes leading to the observed phenomena once their consistency

✉ M. Schüssler
schuessler@mps.mpg.de

[1] Kiepenheuer-Institut für Sonnenphysik, Schöneckstr 6, 79104 Freiburg, Germany

[2] Institute of Theoretical Astrophysics, University of Oslo, P.O. Box 1029 Blindern, 0315 Oslo, Norway

[3] Max-Planck-Institut für Sonnensystemforschung, Justus-von-Liebig-Weg 3, 37077 Göttingen, Germany

[4] School of Space Research, Kyung Hee University, Yongin, Gyeonggi-Do, 446-701, Republic of Korea

with the observations is shown by comparing 'synthetic' with real observations. The simulations then can sharpen the questions addressed by the observations by predicting further properties of the magnetic, thermodynamic, and flow structure.

In this review, we consider a subset of the solar magnetoconvective phenomena, also focussing on more recent developments. Plage and network fields are of considerable interest, not only because of their intrinsic importance for understanding the interaction of magnetic field and convective flows at various spatial scales, but also because of their crucial role for solar irradiance variations with potential impact on terrestrial climate variations. Internetwork fields in the 'quiet' Sun probably represent a huge reservoir of restless 'turbulent' magnetic flux, possibly heralding a fully magnetized state (in the sense of equipartition between magnetic and kinetic energy of the convective motions) of the whole convection zone with important implications for the solar dynamo and the generation of differential rotation. A plausible mechanism for the generation of the internetwork field is small-scale dynamo action by a flow with chaotic streamlines, a truly 'turbulent' dynamo. Numerical simulations suggest that such a dynamo could be active throughout the convection zone, but these simulations can only be run for effective Reynolds numbers and magnetic Prandtl numbers far away from solar values. Nevertheless, state-of-the-art radiative 3D-MHD simulations provide results which are consistent with observations. In what follows, we give an overview of the state of research in the three areas mentioned above: plage and network fields (Sect. 2), internetwork fields (Sect. 3), and small-scale dynamo (Sect. 4).

2 Plage and Network Fields

2.1 General Properties of Plage and Network Fields

At photospheric layers active regions are mainly composed of large, cool magnetic features such as sunspots and pores and smaller, bright magnetic elements forming the plage regions, named after the bright appearance of such regions at chromospheric heights. They are sometimes also called facular fields after the bright faculae visible mainly near the limb in white light (or in other photospheric continuum radiation). Similarly, network features are named after the network of brightenings seen in the cores of chromospheric lines and covering the quiet Sun.

Plage and network magnetic fields are intermediate between the large and dark sunspots and pores on the one hand, and the small weak internetwork magnetic features on the other hand. They are distinguished from the pores by the fact that they are considerably brighter in white light, being on average roughly the same brightness as the average quiet Sun (around solar disc centre), or brighter (near the limb). Their larger magnetic fluxes and their arrangement inside active regions or at the boundaries of supergranule cells distinguishes them from the internetwork elements.

Earlier reviews covering the physics of photospheric flux tubes and in particular plage and network magnetic fields have been written by Solanki (1993); Stenflo (1994); Solanki et al. (2006); de Wijn et al. (2009); see also Stein (2012) for a review of magnetoconvection, which is central to the physics of faculae and the network, and Wiegelmann et al. (2014) for a more recent overview of magnetic fields in the solar atmosphere, but focusing more on the corona.

Plage and network magnetic fields are distinguished from each other by the fact that the density of magnetic flux typically present inside plage is higher, and by their location, with the former being found inside active regions, while network fields are present all over

the Sun (including among the decay products of active regions, which form the so-called enhanced network), but concentrated mainly at the edges of supergranules with a length scale of 15–30 Mm. This implies that the plage fields are restricted to the activity belts, i.e. to latitudes lower than roughly ±30° (see Hale and Nicholson 1925), while the network is seen at all latitudes (Muller and Roudier 1994). In addition, plage and network show a markedly different behaviour over the solar activity cycle, with the solar surface area covered by plage regions waxing and waning strongly in phase with the number of sunspots, while the network fields display a much weaker variation with time. Indeed, there is some controversy about the extent to which network fields vary in phase or in antiphase with the solar cycle (Harvey 1993; Harvey and Zwaan 1993; Hagenaar et al. 2003). Jin et al. (2011) have proposed that the phase vs. anti-phase behaviour depends on the size and flux of the network magnetic features, with the larger features varying in phase, while the smaller features vary in antiphase with the sunspot cycle.

Also, plage and network fields have partly different origins. A large fraction of the plage fields emerge in place, but some are the decay products of the sunspots in their active regions (Petrovay et al. 1999). Therefore, plage fields are generally produced by the global dynamo. The network in turn is partly the result of the decay of active region plage. To a larger extent, however, the network is fed by ephemeral regions, also called ephemeral active regions, small bipolar regions without sunspots with magnetic fluxes of roughly 10^{18}–10^{20} Mx (Dodson 1953; Harvey and Harvey 1973; Harvey and Martin 1973).

The constant emergence of new magnetic flux in the form of ephemeral regions over the solar surface, at a rate of 3×10^{21} Mx per hour (assuming a homogeneous emergence rate over the entire Sun; Schrijver et al. 1997), implies a constant removal of magnetic flux at the same rate. This has led to estimates of the flux turnover time in the magnetic network of 40 h by Schrijver et al. (1998) and 14 h by Hagenaar (2001).

Recently, the importance of the contribution to the network by magnetic flux emerging in the intranetwork has been pointed out (Gošić et al. 2014). Although both, merging and cancellation processes take place (Iida et al. 2012), the former was found to strongly dominate, resulting in a rate of net flux transfer of 1.5×10^{24} Mx per day from the internetwork to the network. Gošić et al. (2014) argue that this implies internetwork fields replace the entire flux in the network within 18–24 hours, on the same order as the replacement time deduced by Hagenaar (2001) based on ephemeral regions. The authors do not discuss the pressing question of why, if the internetwork flux in the two polarities is well balanced while the network flux in their observations clearly is not, merging dominates so strongly over cancellation. Also unclear is what happens with the internetwork flux of the opposite polarity, which is not merged with the network. Also unclear is why, if the flux contributed by the internetwork to the network is an order of magnitude larger than that contributed by ephemeral regions, the turnover times for the network flux found by Hagenaar (2001) (based only on ephemeral regions) is similar to that obtained by Gošić et al. (2014) (including also internetwork features). This could imply that the network in the region considered by Gošić et al. (2014) carried a particularly large amount of flux. Furthermore, the decay or fragmentation of network elements provides an additional source of internetwork flux, so that the net contribution of the internetwork to the network field could actually vanish.

2.2 Observations of Magnetic Concentrations Making Up Plage and the Network

In photospheric layers, where most of the measurements of solar magnetic fields have been made, both, plage regions and the network are composed of groups of more or less discrete magnetic flux concentrations. These concentrations display a range of sizes

(e.g. Utz et al. 2009; Feng et al. 2013) and magnetic fluxes, whose probability distribution function follows a power law with an exponent of -1.85 according to Parnell et al. (2009), or -2 according to Harvey and Zwaan (1993). These values indicate that large and small magnetic concentrations contribute roughly the same amount to the total unsigned magnetic flux present at any given instant on the solar surface (with the larger features dominating if the value of Parnell et al. 2009 is used). Owing to the much shorter lifetime of ephemeral regions, this approximate equality implies they bring magnetic flux to the solar surface at a much higher rate than the larger active regions. Zirin (1987) has estimated that there is a factor of 100 difference in the fluxes emerging over a solar cycle in these two types of bipolar features (cf. Thornton and Parnell 2011; Zhou et al. 2013).

Magnetic fields in active regions and the network are mainly strong, i.e. on the order of 1–2 kG (Stenflo 1973; Wiehr 1978; Dara-Papamargaritis and Koutchmy 1983; Rabin 1992a; Rabin 1992b; Rüedi et al. 1992b; Grossmann-Doerth et al. 1996; Martínez Pillet et al. 1997; Sánchez Almeida and Lites 2000; Viticchié et al. 2011; Bühler et al. 2015), also see Blanco Rodríguez and Kneer (2010) and Kaithakkal et al. (2013) for polar faculae. These fields are close to vertical (e.g., Sanchez Almeida and Martinez Pillet 1994; Bernasconi et al. 1995; Martínez Pillet et al. 1997; Bühler et al. 2015); cf. Leighton (1959), albeit with limitations of their instrument at the time. Note that the field strength is a strong function of height, dropping from high values of around 1500–2000 G in the deepest observable layers (Rabin 1992a; Rüedi et al. 1992b; Bühler et al. 2015) to a field strength of 250–500 G in the upper photosphere (Zirin and Popp 1989; Bruls and Solanki 1995; Bühler et al. 2015); see also Moran et al. (2000). In addition to the kG flux concentrations, small patches of transient horizontal field are also found in active regions (Ishikawa et al. 2008; Ishikawa and Tsuneta 2009), with properties that are similar to corresponding patches in the quiet Sun. In particular, the smaller ones are isotropically oriented, although the larger ones appear to have a slight preference for the orientation of the active region.

According to Abramenko and Longcope (2005) magnetic flux concentrations within active regions possess fluxes of 10^{18}–10^{20} Mx, whereby features with fluxes larger than 10^{19} Mx are likely darker than the surroundings (e.g., Grossmann-Doerth et al. 1994). The network is composed of smaller magnetic features hosting less magnetic flux, with kG flux tubes carrying a flux of around 10^{17} Mx being the smallest such entities that have been isolated so far. Even smaller magnetic features are regularly seen in radiation MHD simulations and are also likely to be present on the Sun. Solanki et al. (1999) pointed out that magnetic features with magnetic fluxes differing by up to 6 orders of magnitude have roughly the same field strength of 1000–2000 G when averaged over their cross-sections. Such magnetic features range from the smallest kG flux tubes (magnetic elements) to large sunspots. Note that only the field strength averaged over the whole cross-section remains roughly independent of magnetic flux, the field strength at the core of the features changes by a considerable amount. Magnetic features with flux below a few times 10^{16} Mx have weaker fields (e.g. Solanki et al. 1996; Khomenko et al. 2003; Orozco Suárez et al. 2008; Ishikawa and Tsuneta 2009; Stenflo 2011; Utz et al. 2013). Note that the field strength of individual magnetic structures may also be a function of time, e.g. emerging magnetic flux is usually associated with a weaker field (e.g. Zwaan 1985; Zhang and Song 1992; Lites et al. 1998; Centeno et al. 2007; Martínez González and Bellot Rubio 2009; Cheung and Isobe 2014), but in small features the field strength may also vary significantly after that (e.g. Martínez González et al. 2011a; Requerey et al. 2014).

The strong magnetic fields in plage decrease the convective blueshift of spectral lines (Livingston 1982; Cavallini et al. 1985; Brandt and Solanki 1990) in agreement with

the smaller upflow velocities in granules along with the faster downflows in intergranular lanes seen by Kostik and Khomenko (2012). These authors also find that the convective flows reach greater heights in facular areas. The contrast of the granulation and the sizes of individual granules become smaller in plage while their lifetimes increase, resulting in what is called abnormal granulation (Title et al. 1992; Berger et al. 1998; Narayan and Scharmer 2010).

Martínez Pillet et al. (1997) noted from Stokes vector observations with a spatial resolution of around 1 arc sec obtained with the Advanced Stokes Polarimeter (ASP) that the magnetic concentrations in plage displayed no significant downflows beyond about 250 m/s, confirming a result first found by Solanki (1986). The absence of downflows was later challenged by Bellot Rubio et al. (2000), who argued that the tiny wavelength shifts of the many lines in a Fourier-Transform-Spectrometer (FTS) Stokes V spectrum could only be interpreted in terms of a strong downflow inside the magnetic features. This was in turn criticised by Frutiger and Solanki (2001), who showed that this signature could also be produced by velocities not requiring a net flow. Consequently, spatially unresolved data have not been able to provide a definitive answer to the question of flows within magnetic elements. Upflows of around 1–2 km/s inside plage magnetic elements, surrounded by 1.5–3.3 km/s downflows, were reported by Langangen et al. (2007). Recently, Bühler et al. (2015) have confirmed the location of the magnetic concentrations inside the downflow lanes separating granules, but without harbouring strong downflows themselves. At individual locations up- and downflows within the magnetic features are present, but in an average sense they are close to being at rest. These authors also discovered that the downflows immediately surrounding strong flux concentrations can reach supersonic values at the solar surface, unlike in normal intergranular lanes, which display only subsonic downflows in similar data. This provides observational confirmation that the additional cooling of the gas in the immediate surroundings of magnetic concentrations causes the surrounding gas to sink faster, as initially pointed out by Deinzer et al. (1984).

An early discovery of the observation of full Stokes V profiles was their asymmetry. The blue and red wings of the profiles having different amplitudes and areas (Stenflo et al. 1984; Solanki and Stenflo 1984; Solanki and Stenflo 1985), with the asymmetry being in general larger in network features than in plage. Stenflo et al. (1987) found the sign of the area asymmetry to change near the solar limb. These results were confirmed by Martínez Pillet et al. (1997) for plage regions. The Stokes V area asymmetry has been interpreted in terms of (nearly) static gas inside flux tubes whose field expands with height thus forming a canopy overlying the downflowing lanes of the surrounding convective cells (Grossmann-Doerth et al. 1988; Solanki 1989; Steiner et al. 1999; Shelyag et al. 2007). This geometry is now well-established and easily visible in high-resolution images (Berger et al. 2004; Pietarila et al. 2010), see also the previous paragraph. This picture could also explain the change in sign of the asymmetry close to the limb (Bünte et al. 1993) and high resolution observations that show Stokes V to be less asymmetric in the interiors of magnetic concentrations, but strongly asymmetric near the edges, i.e. where the canopy is expected to be located (Rezaei et al. 2007; Martínez González et al. 2012b). Rezaei et al. (2007) even find an opposite sign of the asymmetry inside magnetic features in the examples considered by them. Such observations are a sign that magnetic flux concentrations in plages and the network are becoming spatially resolved and their internal structure probed. Some Stokes V profiles are anomalous in shape, i.e. having only a single lobe, or three or four lobes. Such profiles are most common in the internetwork of the quiet Sun, but are to some extent also found in active-region plage. They can have different origins, with Sigwarth (2001) proposing network and plage fields as either a mixture of kG flux tubes and a sub-kG field.

This interpretation is supported by high resolution observations that indicate weak opposite polarity fields surrounding kG magnetic features.

Martínez Pillet et al. (1997) also found that plage fields contain many so-called azimuth centers, i.e. regions where, starting from the center of the feature, the magnetic azimuth points roughly isotropically in all horizontal directions. They are thought to be signatures of intermediate-sized magnetic features described by flux tubes expanding with height. Inversions of data obtained by Hinode by Bühler et al. (2015) have confirmed the presence of numerous azimuth centres in plage areas. These authors also showed that the larger of these are associated with micropores. Also visible are weak opposite polarity fields located just outside the magnetic features in the deepest observable layers, underlying the canopy of expanding fields in the upper photosphere (Zayer et al. 1989; Narayan 2011; Scharmer et al. 2013; Bühler et al. 2015).

2.3 Brightness of Magnetic Features in Plage and the Network

The brightness of magnetic concentrations in plage and the network has been a subject of intense study. The brightness gives insight into the transport of energy within magnetic features, e.g., by the influx of radiation from the surrounding granules (e.g. Spruit 1976; Stenholm and Stenflo 1977; Vögler et al. 2005; Holzreuter and Solanki 2012). Another strong motivation comes from the contribution of facular and plage brightness to changes in the total and spectral solar irradiance, the solar drivers of the Earth's climate (e.g. Foukal et al. 2004; Domingo et al. 2009; Gray et al. 2010; Ermolli et al. 2013; Solanki et al. 2013) along with other natural and man-made causes. Until recently the highest spatial resolution was reached only, or at least the easiest, in broad-band images taken in rapid bursts.

The variation over the solar cycle of solar surface area coverage by plage also changes the intensity close to the solar limb (due to the enhanced brightness of plage there) and hence produces variations in the apparent solar radius (Bruls and Solanki 2004, cf. Ulrich and Bertello 1995).

The contrast of magnetic elements with respect to the quiet Sun increases rapidly with height in the photosphere (e.g. see Riethmüller et al. 2010). At the height of formation of the continuum in visible light the contrast is low and can be of either sign. It is generally much stronger at higher layers, sampled by, e.g., line cores (e.g. Title et al. 1992; Stangl and Hirzberger 2005; Yeo et al. 2013). The continuum and line core contrasts also display a totally different centre-to-limb behaviour. In the continuum the contrast is low at disk centre. According to Topka et al. (1992, 1997) it is even negative for all types of magnetic features. Negative contrasts of some types of small-scale magnetic features have also been seen by Ortiz et al. (2002); Berger et al. (2007); Yeo et al. (2013). The continuum contrast increases toward the solar limb (Domingo et al. 2005; Kobel et al. 2009). Such a behaviour is also observed for polar faculae (Blanco Rodríguez et al. 2007). In many observations, the continuum contrast increases from disk centre only up to a given heliocentric angle (θ), and then decreases towards the limb. Thus Auffret and Muller (1991) find that it peaks at around $\mu = \cos\theta \approx 0.35$, while Ortiz et al. (2002) and Yeo et al. (2013) obtain that this angle depends on the average flux density, i.e. probably the size of the magnetic feature, which is in good agreement with results from flux-tube models.

In line cores, however, the largest contrasts are found near solar disk centre, with the contrast decreasing towards the limb (Yeo et al. 2013). Hirzberger and Wiehr (2005) found no significant variation of the contrast of faculae with heliocentric angle, from observations in G-band and 587.5 ± 1.5 nm continuum. In the G-band this can be explained by the mixture of lines and continuum, at 587.5 nm, it is more surprising.

The continuum contrast of magnetic elements is, on average, larger in the network than in the plage (Ortiz et al. 2006; Kobel et al. 2011; Romano et al. 2012). This is mainly caused by the larger average size of magnetic elements in these regions, with magnetic features in plages being larger on average (Grossmann-Doerth et al. 1994). Larger features are generally less bright around disk centre.

Correspondence of localised brightness enhancements to the magnetic flux concentrations have been shown in MHD simulations (Vögler et al. 2005; Shelyag et al. 2007) as well as in the observations. Observations at solar disc centre display a decrease in the contrast of magnetic features with field strength, either starting right from small field-strength values (Topka et al. 1992, 1997; Title et al. 1992), or after an initial increase, i.e. displaying a "knee" in brightness (Lawrence et al. 1993; Stangl and Hirzberger 2005; Narayan and Scharmer 2010; Schnerr and Spruit 2011; Kobel et al. 2011). Note, however, that observations made by Schnerr and Spruit (2011) with the very high resolution SST (Swedish Solar Telescope; Scharmer et al. 2003) display an increasing brightness right up to the largest field strengths that they plot. This suggests that the spatial resolution does play a role in the relationship between brightness and magnetic flux. Danilovic et al. (2013) studied the effect of degrading simulated images to the spatial resolution of Hinode/SP images (i.e. of limiting the spatial resolution; see also Röhrbein et al. 2011). With the help of the appropriate point-spread-function Danilovic et al. (2013) could reconcile the different rms contrasts obtained from MHD simulations and observations. The apparent difference between the contrast of magnetic features in observations and MHD simulations was pointed out and explained by Röhrbein et al. (2011). They showed that the application of an appropriate point-spread-function turned the monotonic relation between brightness and field strength found at the original resolution of their MHD simulations into a relation with a maximum at intermediate field strength.

A very high contrast is achieved by imaging within molecular bands, which have the advantage that owing to the large density of lines, relatively broad filters can be used, allowing a good signal-to-noise ratio to be reached within a short exposure time. The most commonly used molecular band has been the Fraunhofer G-band of CH molecular absorption (Muller and Roudier 1984; Muller and Mena 1987; Berger et al. 1995; van Ballegooijen et al. 1998; Berger and Title 2001; Nisenson et al. 2003; Langhans et al. 2004; Rouppe van der Voort et al. 2005; Viticchié et al. 2010; Bodnárová et al. 2014). The bright points seen in this wavelength range are associated with magnetic fields (Berger and Title 2001; Bharti et al. 2006; Beck et al. 2007), though not all areas with a large magnetic flux can be necessarily associated with G-band bright points (Ishikawa et al. 2007). Although the CN-bandhead at 388 nm offers a larger density of lines and hence produces stronger contrasts (e.g. Rutten et al. 2001; Berdyugina et al. 2003; Zakharov et al. 2005; Uitenbroek and Tritschler 2007; but see Uitenbroek and Tritschler 2006 for a deviating view), the G-band profits from the often higher camera sensitivity and the larger number of solar photons. The high contrast of the molecular bands comes from the dissociation of the CH (respectively the CN) molecule in the higher temperature of magnetic elements (Steiner et al. 2001; Sánchez Almeida et al. 2001), which is well reproduced by radiation-MHD simulations (Schüssler et al. 2003; Shelyag et al. 2004).

A small portion of an active region is imaged in the photospheric G-band and the low chromospheric passband centred on the Ca II H line core in Figs. 1A and 1B, respectively (from hight-resolution observations with SST; from Berger et al. 2004). They clearly demonstrate the increasing contrast with height. The Fe I 630.25 nm magnetogram is displayed in Fig. 1C, for comparison with the location of the bright points. Also, Fig. 1D presents the corresponding Dopplergram linearly scaled between -1.5 and 0.8 km/s.
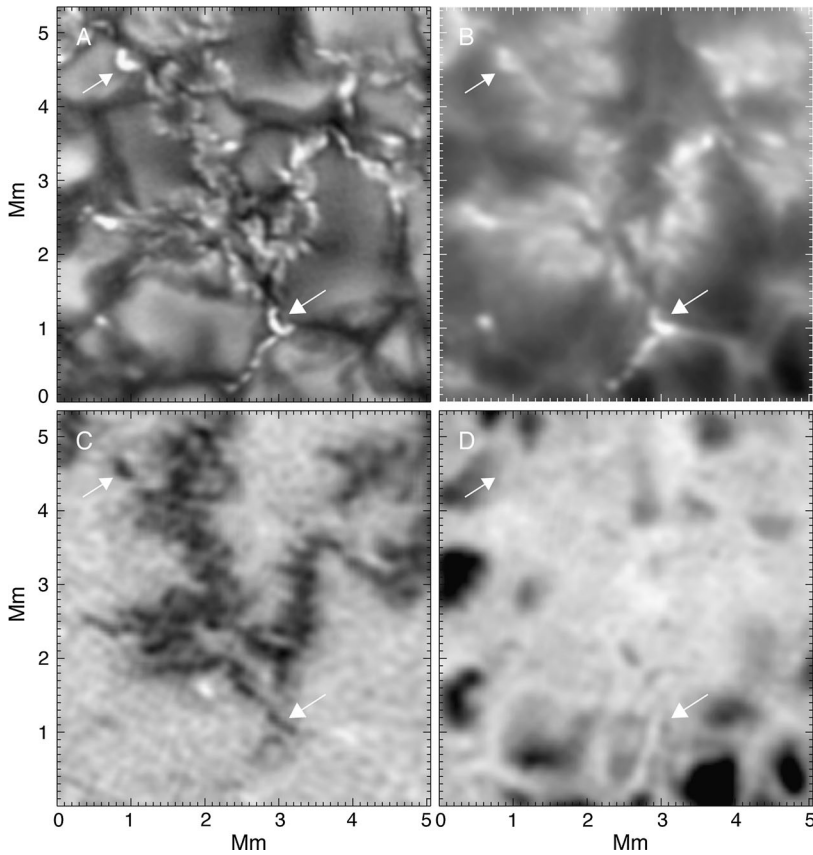
Fig. 1 Brightness contrast in G-band (**A**) and Ca II H (**B**) passbands, from high-resolution observations with SST, as well as maps of magnetic flux density (**C**) and of line-of-sight velocity (**D**). The magnetic flux density and the line-of-sight velocity are linearly scaled, ranging from -1090 to 330 Mx/cm^2 and from -1.5 to 0.8 km/s, respectively. The *arrows* indicate loop-like emission structures over downflowing lanes studied by Berger et al. (2004) (see Sect. 2.2). Reproduced with permission from Berger et al. (2004), Astronomy & Astrophysics, © ESO

The main difference between plage and network magnetic features is their size (e.g. Kobel et al. 2014), i.e. the amount of magnetic flux that they carry, as well as their motions. The brightest magnetic elements may have, however, similar sizes in plage and the network (Kobel et al. 2011). Some of the other differences are probably related to the size difference. An example is their lifetimes, which are likely to be different in the network and in plage, since larger magnetic features tend to live longer (Meunier and Zhao 2009).

A number of studies have found a correlation between the intrinsic field strength of magnetic elements in network and plage and the magnetic filling factor, which is a proxy of the amount of magnetic flux in a given spatial resolution element (Stenflo and Harvey 1985; Schüssler and Solanki 1988; Zayer et al. 1990; Keller et al. 1990; Rüedi et al. 1992b; Grossmann-Doerth et al. 1996; Martínez Pillet et al. 1997; Sigwarth et al. 1999). In most of these studies the resolution element was considerably larger than the individual magnetic features. The dependence may, again, be related to the larger average size of magnetic features in regions with higher magnetic flux density.

Fig. 2 Sketch of the vertical cross-section of a thin flux tube (*shaded*, *gray*). The Wilson depression, ΔZ, is the geometrical difference between the same optical depth ($\tau_{5000} = 1$) inside and outside of the flux tube (see main text). The radiating hot walls are indicated by *yellow blocks*. The *green arrows* illustrate the convection. The cartoon is not to scale. Inspired by a similar sketch by Schrijver and Zwaan (2000)
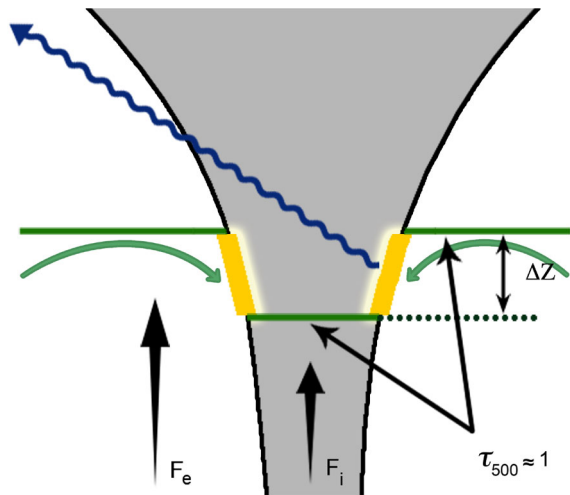
2.4 Theoretical Description of Plage and Network Magnetic Concentrations

Solar magnetic flux concentrations have generally been described by a flux-tube model (see, e.g., Spruit 1976, 1977, 1981; Deinzer et al. 1984; see Solanki 1993, for a review of early work). It assumes that the magnetic features can be described by a bundle of ordered field lines that are enclosed by a topologically simple surface. In addition, the features are assumed to be stationary and in force and energy balance with their surroundings. Although reality is expected to be more complex than this, for many purposes further simplifications are introduced. For example, the shape of the cross-section of (vertical) flux tubes is often considered to be round (i.e. having axial symmetry). This geometry also builds on the near axial symmetry of the most regular sunspots. Alternatively, sometimes flux sheets, with translational and mirror symmetry, are considered (e.g., Holzreuter and Solanki 2012). This geometry describes better magnetic structures in regions with a larger concentration of magnetic flux as in active-region plage. There the flux has a tendency to fill the intergranular lanes, i.e. to concentrate into "ribbon-like" structures (Bushby and Houghton 2005). In general, it is assumed that a flux tube (used as a generic term also to describe features with a non-circular cross-section) are surrounded by an electric current layer where the magnetic field drops rapidly. The width of this layer is estimated to be a few km (Schüssler 1986).

A further and very commonly used simplification is the thin-tube approximation (Parker 1955; Defouw 1976; Pneuman et al. 1986; Ferriz-Mas et al. 1989). In its simplest form it reduces force balance to a simple horizontal and vertical balance of the total pressure (composed of gas and magnetic pressure, with sometimes the inclusion of turbulent pressure as well, which, however, is small compared to the other two in the solar photosphere). The assumption is strictly valid only for flux tubes whose radii are much smaller than the pressure scale height (which in the photosphere is on the order to 100 km). Due to the presence of magnetic pressure inside the tube, the gas pressure and hence also the density is lower there, so that we see deeper layers (an effect known as the Wilson depression in sunspots, where it can be directly observed; e.g. see Solanki 2003 for a review; also Lites et al. 2004 for observations at high spatial resolution).

A sketch outlining the main points of a photospheric flux tube is given in Fig. 2. It illustrates a typical, small-scale magnetic flux concentration that appears bright. The evacuation inside the flux tube lowers the optical depth inside the tube (Wilson depression) allowing the

radiation from the hotter gas inside the tube (compared to the external gas at equal optical depth although not necessarily at equal geometric height) to escape and hence be observed. The gas inside the tube is heated by radiation from the hot walls of the tube (yellow in the sketch) through which the hot sub-surface gas in the surroundings radiates excess energy, compared to the surroundings intergranular areas (Spruit 1976).

Convective energy transport is strongly reduced or completely quenched by the strong magnetic field inside magnetic flux tubes with kG fields (Gough and Tayler 1966; Ferriz-Mas and Schüssler 1994). Since the vertical energy transport by radiation is comparatively inefficient in the solar convection zone, for $\tau \gg 1$ the vertical energy flux density inside the flux tube, F_i, is much smaller than that in the surroundings, F_e. Consequently, most of the energy influx into the interior of a flux tube comes through radiation flowing in from its walls (between the $\tau = 1$ levels inside and outside the flux tube), as originally proposed by Spruit (1976) and later demonstrated with the help of numerical simulations by, e.g., Deinzer et al. (1984); Knoelker and Schüssler (1988); Vögler et al. (2005), cf. Schrijver and Zwaan (2000).

As the gas pressure drops with height, so must the magnetic field in order to maintain pressure balance. Magnetic flux conservation then causes the magnetic field to expand with height, creating a canopy of field overlying the convecting gas. Above a certain height the field of neighbouring magnetic features reaches each other and if they are of the same polarity (which is common in active region plage), they merge (Spruit 1983). The rate of expansion of the field is given mainly by the relative temperature inside and outside the flux tube (Solanki and Steiner 1990). We note that the relative rates of expansion with height of large and small flux tubes are similar (Solanki et al. 1999).

The MHD simulations clearly show that the magnetic flux concentrations are neither mainly circular, nor always sheet-like (although examples of features similar to both types can be found, see Figs. 3 and 4). Rather they constantly evolve, changing in size and shape, and interact with each other. Although the shape of the cross-section does not agree with that underlying the thin-tube approximation, the main assumption, namely of horizontal pressure balance, turns out to be satisfied if the second order expansion of the thin-tube approximation, as derived by Pneuman et al. (1986) and Ferriz-Mas et al. (1989), is used (see Yelles Chaouche et al. 2009). Figure 3 presents results of the MHD simulations by Yelles Chaouche et al. (2009), where the vertical component of the magnetic fields, gas pressure, and total pressure are plotted for three different photospheric layers, with $z = 0$ corresponding to the spatially averaged optical depth unity at 500 nm.

2.5 Comparison of Theory and Observations

How does the model of the thin flux tube (or flux sheet) live up to observations? One great success of this model has been that it could reproduce the centre-to-limb variation of the brightness of magnetic features (or equivalently of their contrast relative to the quiet Sun).

Now, thanks to the high-resolution data available from sources such as Hinode (Tsuneta et al. 2008), the Swedish Solar Telescope (Scharmer et al. 2003) and the Sunrise balloon-borne observatory (Solanki et al. 2010; Barthol et al. 2011; Berkefeld et al. 2011; Gandorfer et al. 2011; Martínez Pillet et al. 2011) we can test with much higher fidelity to what extent such descriptions live up to reality.

Thus, the presence of weak opposite-polarity fields surrounding magnetic flux concentrations has been established by MHD simulations, as can be seen in Fig. 4 taken from Vögler et al. (2005), in good agreement with the observations of such fields (Zayer et al. 1989; Narayan 2011; Scharmer et al. 2013; Bühler et al. 2015). The simulations reveal the geometry of the opposite polarity fields (which is not accessible to the observations). These fields
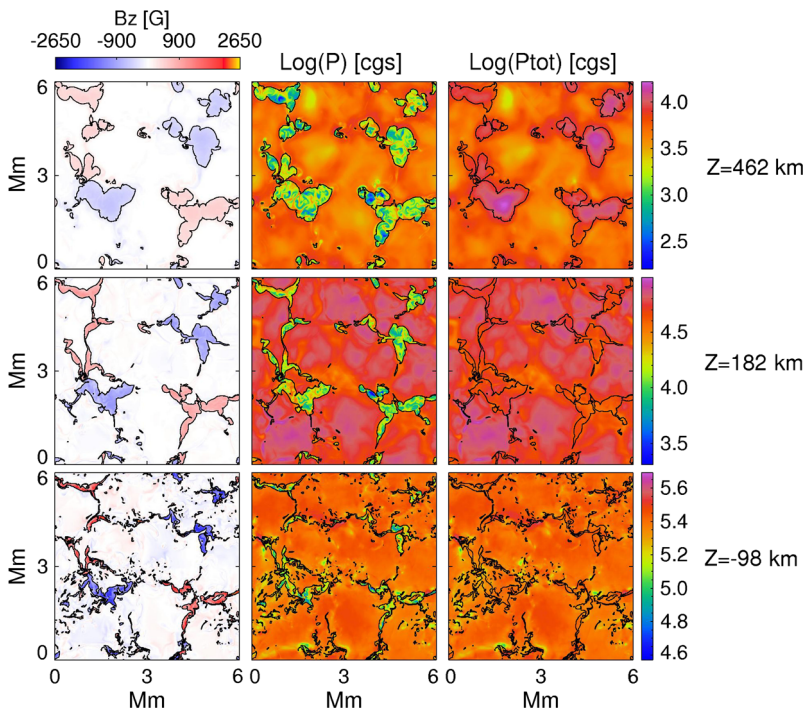
Fig. 3 Stratification of the longitudinal component of the magnetic field (B_z; *left column*), gas pressure (P; *middle column*), and total pressure ($Ptot$; *right column*), with respect to the optical depth unity at 500 nm. The *black contours* include areas where $|B_z| > 500$ G at -98 km, $|B_z| > 400$ G at 182 km, and $|B_z| > 300$ G at 462 km. Reproduced with permission from Yelles Chaouche et al. (2009), Astronomy & Astrophysics, © ESO

are due to field lines anchored within the magnetic concentration that are turned over and pulled down by the surrounding downflows. In general, they do not extend higher up in the atmosphere, but rather most of these turn back at relatively low heights in the photosphere, just as in the observations. Illustrated in Fig. 5 is a side-view of such structures from MHD simulations (Vögler et al. 2005), where concentrations of the field lines represent along-side-view of a thin magnetic sheet, surrounded by the low-lying field lines.

A remarkable success of MHD simulations has been the agreement of the brightness (or brightness contrast) of simulated magnetic features with that of observed ones. The centre-to-limb variation of the contrast at various wavelengths has been modelled by Carlsson et al. (2004), Keller et al. (2004), and Penza et al. (2004), cf. Steiner (2005). The distribution of the brightness of magnetic bright points in the G- and CN-bands has been successfully compared with the high-resolution Sunrise observations by Riethmüller et al. (2010). The RMS contrast in the same images is dominated by granulation and was also reproduced by the same simulations (Hirzberger et al. 2010). Riethmüller et al. (2014) went a full step further and compared not just the brightness in broad wavelength bands, but also a host of further parameters, such as the Stokes V amplitude, the Doppler shift, the line width, etc. and found a good agreement (with some slight disagreement only in the width of the distribution of Doppler shift values) between the values found in the quiet Sun by Sunrise and those from an MHD simulation with an average vertical field of 30 G. The evolution of the fine-structure of faculae has been investigated by, e.g., De Pontieu et al. (2006), who
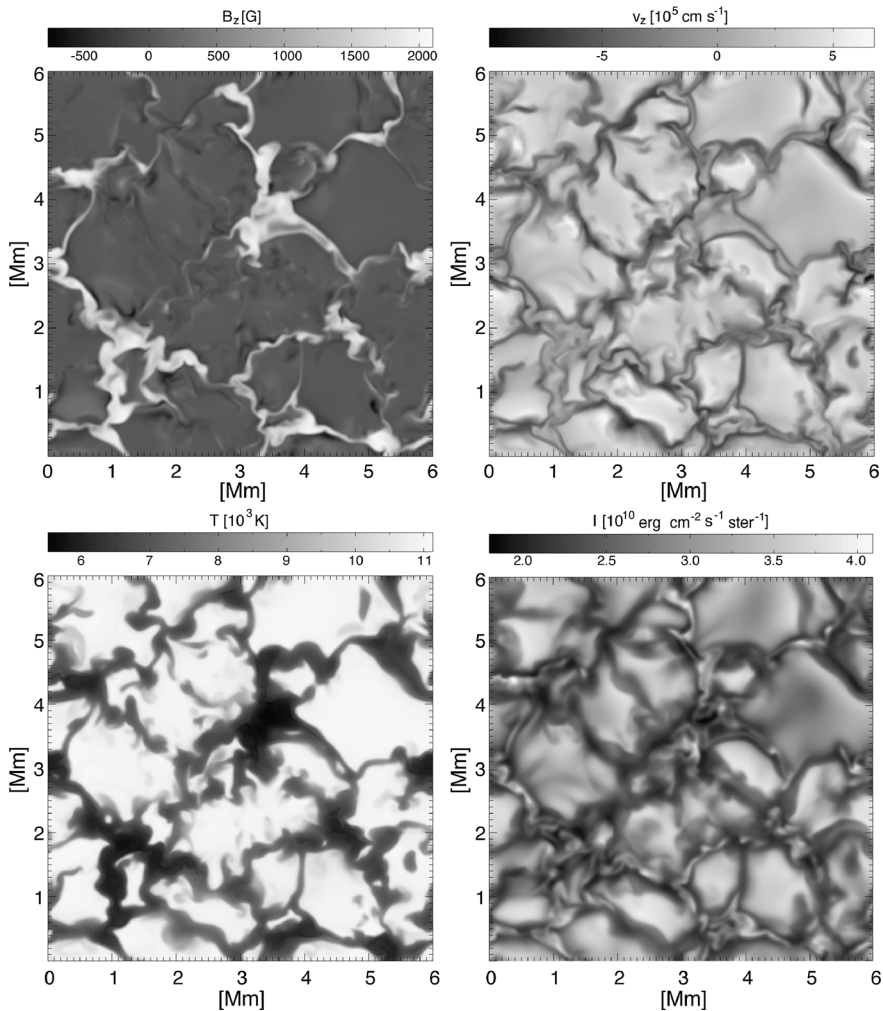
Fig. 4 Maps of longitudinal magnetic field (*upper left*), line-of-sight velocity (*upper right*), temperature (*bottom left*), and intensity (*bottom right*) at the average geometrical height corresponding to optical depth unity (at 500 nm), from MHD simulations made with the MuRAM code. The strong magnetic field concentrations, in downflow areas, are surrounded by narrow lanes of weak opposite-polarity magnetic flux. Reproduced with permission from Vögler et al. (2005), Astronomy & Astrophysics, © ESO

found, using both high-resolution observations and MHD simulations, that faculae change on a time-scale of minutes and that this change is mainly produced by the evolution of the granules lying just behind them, whose hot sides are better seen due to the evacuation of the faculae.

Disagreements in the observed and simulated rms contrasts found by, e.g., Uitenbroek et al. (2007), are very likely due to the effect of scattered light that is pervasive in ground-based data and even affects space-based observations (Danilovic et al. 2008). The best observations with low scattered light, e.g., Hirzberger et al. (2010), display a good agreement with simulated rms contrasts. These results indicate the importance of the scattered light in decreasing the contrast of high-resolution observations.

Fig. 5 A side-view from MHD simulations, illustrating geometry of the field lines at magnetic flux concentrations (along a thin magnetic sheet) surrounded by weaker low-lying magnetic loops. The *grey plane* indicates the average geometrical height corresponding to $\tau_{5000} = 1$. Reproduced with permission from Vögler et al. (2005), Astronomy & Astrophysics, © ESO
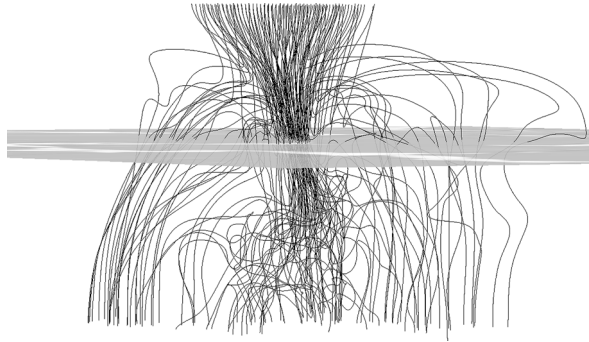
2.6 Concentration of Magnetic Flux: Convective Collapse

The formation of strong-field magnetic features was for a long time studied mainly with theoretical methods. Two main mechanisms for the concentration of magnetic flux were proposed. The first, flux expulsion, represents a self-organized separation of magnetic field from convection. Any vertically oriented magnetic field at the solar surface is quickly transported to the intergranular lanes by the horizontal flows within granules. This allows granular convection to continue operating even in the presence of a significant amount of magnetic flux (although the convection cells do change, becoming smaller, less turbulent with smaller horizontal velocities, as well as more ordered with a longer lifetime, e.g. Title et al. 1989, 1992; Narayan and Scharmer 2010). The fields produced by this mechanism have roughly the same energy density as the convective flows (i.e. the field is in equipartition with the kinetic energy of the flow), which corresponds to roughly 200–400 G at the solar surface.

The convective instability, acting on regions with such equipartition fields can then intensify them to kG levels (Parker 1978; Webb and Roberts 1978; Spruit 1979; Spruit and Zweibel 1979; Schüssler 1990; Takeuchi 1997; Grossmann-Doerth et al. 1998; Steiner 2003; Danilovic et al. 2010b; Hewitt et al. 2014). The process can be idealized by the adiabatic instability of a static thin magnetic flux tube with an equipartition magnetic field embedded in a superadiabatically stratified medium. The instability leads to accelerated downflow along the tube, which entails a reduction of the internal gas pressure. The excess pressure in the surroundings then compresses and enhances the field until the magnetic pressure becomes sufficiently large to compensate for the loss of gas pressure and a new equilibrium is reached (see Spruit and Zweibel 1979 for a discussion of the non-linear development of the instability). The final state needs not to be a stationary one, with Hasan (1985) finding an oscillatory end state in his 1D model.

In reality, a static equilibrium with equipartition field will most probably never be realized. Instead, the magnetic flux advected by the horizontal granular flow accumulates in intergranular downflow regions. Once the horizontal flow is suppressed by the growing field strength, the downflow is no longer supplied by these flows, yet continues owing to the superadiabatic stratification and the ongoing surface cooling by radiation. This leads to partial evacuation and growth of the field strength (Schüssler 1990).

The 3D radiation MHD simulations of Danilovic et al. (2010b) and Hewitt et al. (2014) followed all steps of the process from the gathering of flux at the intergranular lanes, followed by an evacuation produced by a downflow and the associated strengthening of the field that then quenches the downflow. The field can get weakened again, in some cases possibly due to the following upflows (Grossmann-Doerth et al. 1998;

Danilovic et al. 2010b), but at least in some cases without the need of an upflow (Hewitt et al. 2014).

If magnetic features are below a certain size (or below a certain amount of magnetic flux) then the radiative exchange of energy with the surroundings becomes strong enough to reduce or to completely compensate for the cooling of the downflowing material, so that the collapse does not occur. Hence according to theory the features with the smallest magnetic flux should possess weak fields (Venkatakrishnan 1986; Solanki et al. 1996; Grossmann-Doerth et al. 1998).

Observations have in general been lagging behind the theory, with the first suggestion of a correlation between the magnetic flux of a feature and its intrinsic field strength being found by Solanki et al. (1996). The observed strengthening of the field was first interpreted as a convective collapse by Bellot Rubio et al. (2001). The increase in the field strength in this case was from 400 G to only 600 G. Larger increases have been obtained by the more recent investigations by Shimizu et al. (2008); Nagata et al. (2008); Fischer et al. (2009); Narayan (2011); Requerey et al. (2014); Utz et al. (2014). The final two papers study the evolution of small magnetic elements in the quiet Sun. They find that, at least for these features with relatively small amounts of flux, the strong-field state does not last very long, with the field strength fluctuating in an almost periodic fashion (cf. Martínez González et al. 2011a). These studies suggest that the evolution of the field strength of the larger and stronger magnetic concentrations making up the bulk of active region plage would be a promising topic of study.

3 Recent Discoveries on Internetwork Magnetic Fields

Despite being much more difficult to detect and measure than magnetic fields in sunspots, plage and network regions, internetwork (IN in what follows) magnetic fields are of great importance for several reasons. Firstly, there is the possibility that a considerable amount of magnetic flux in the Sun's quietest regions (i.e., the internetwork) is provided by a turbulent small-scale dynamo. Since numerical simulations cannot be carried out for the extreme solar values of Reynolds numbers and magnetic Prandtl number (see Sect. 4), observations are indispensable to test the validity of the computational results and possibly prove the existence of small-scale dynamo action. Secondly, the relatively weak internetwork magnetic fields (see Fig. 6) interact in a highly dynamical fashion with convective motions in the solar surface layers. This gives rise to highly interesting small-scale phenomena and convoluted magnetic topologies (Amari et al. 2015). Thirdly, if IN magnetic fields are produced by a small-scale dynamo and considering that at least 90 % of the solar surface is covered by the IN,[1] this would mean that most of the unsigned photospheric magnetic flux does not vary over the 11-year magnetic cycle. This could have important consequences for our understanding of the solar irradiance variations, which contribute to terrestrial climate variations (Solanki et al. 2013; Yeo et al. 2014).

The main question is whether IN magnetic fields do actually arise from a turbulent small-scale dynamo or are leftovers of the magnetic fields from decaying active regions, being spread out over the solar surface by advection due to supergranulation, meridional flow, and differential rotation. Therefore, characterizing the internetwork magnetic fields can be considered as one of the most pressing issues in solar physics.

---

[1]This number should be considered as a lower threshold as sometimes it is not easy to distinguish between strong isolated IN fields and the network.
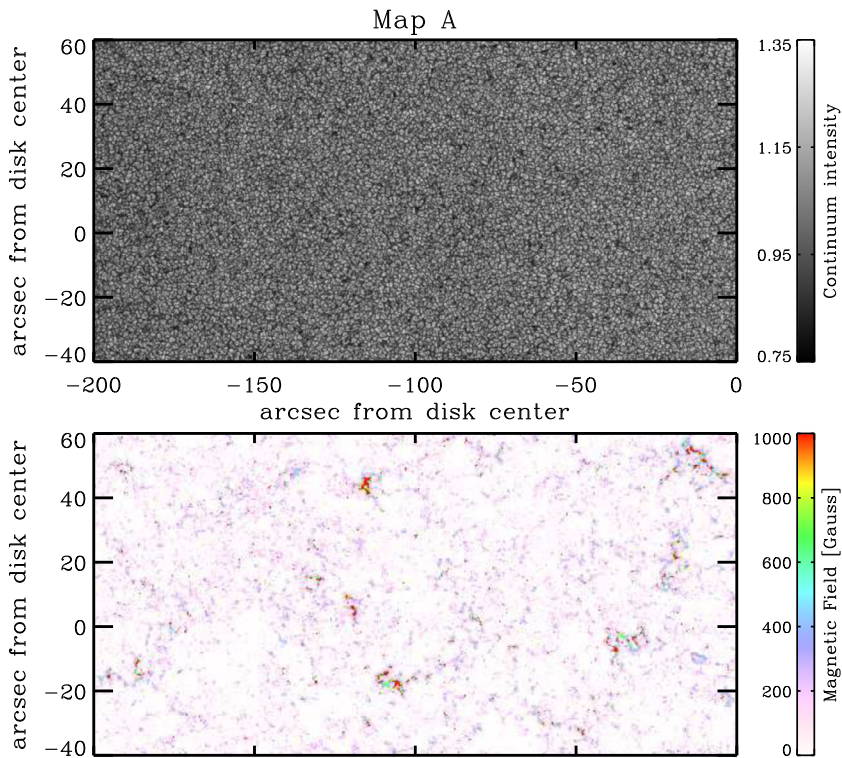
Fig. 6 Continuum intensity normalized to its average value over the entire field of view (*top*) and magnetic field strength (*bottom*) inferred from Hinode observations of the quiet Sun very close to disk center (Borrero and Kobel 2011). The network on the lower map can been identified in *green/orange/red* colors, whereas the internetwork can be seen as the regions in *pink/white* colors. The latter covers at least 90 % of the total observed area. This particular map has been employed by many authors to study the angular distribution of the magnetic field in the internetwork (see Sect. 3.1). Reproduced with permission from Astronomy & Astrophysics, ©ESO

3.1 Angular Distribution of Internetwork Fields

A small-scale dynamo operating in a stratified medium provides an isotropic magnetic field at scales smaller than the pressure scale height. Numerical simulations confirm this expectation in the sub-surface layers, but predict a strong anisotropy in favor of horizontal fields in the photosphere (i.e., in convectively stable layers), both for the small-scale dynamo (Schüssler and Vögler 2008; Rempel 2014) and for magnetoconvection with a mean vertical field (Steiner et al. 2008; Steiner and Rezaei 2012). Consequently, observationally confirming or ruling out such a distribution has been a major field of research over the past decade. Unfortunately, inferring the magnetic field in the internetwork is extremely challenging owing to their weak observational signatures (i.e. polarization signals barely above the noise). Not surprisingly, these difficulties have led to seemingly contradictory results. The situation is further complicated by the varied analysis techniques employed and the different kinds of data analyzed. In the following we present a summary of observational results organized in terms of the inferred angular distribution for IN magnetic fields.

3.1.1 Preference for Horizontal Fields

Orozco Suárez et al. ([2007](#)) and Lites et al. ([2008](#)) analyzed low-noise ($\sigma \approx 3 \times 10^{-4}$)[2] data from the Fe I line pair at 630 nm recorded at disk center with the spectropolarimeter on-board the Hinode satellite. Employing inversion techniques and different calibration curves they concluded that magnetic fields in the internetwork have a clear preference for the horizontal (i.e. parallel to the solar surface) direction, with the horizontal magnetic field being much stronger (in a spatially average sense) than the vertical one. However, Stenflo ([2010](#)) and Borrero and Kobel ([2011](#), [2012](#)) later argued that this result is likely due to photon noise. Indeed, if we consider a weak magnetic field whose projection along the observer's line of sight is the same as the projection on the plane perpendicular to the line of sight, $B_\parallel = B_\perp$, the 630 nm lines provide much smaller (about 10 times weaker) signal in linear polarization (Stokes Q and U) than in circular polarization (Stokes V). Consequently, the same amount of photon noise in the observed circular and linear polarizations is interpreted as a magnetic field with $B_\perp \gg B_\parallel$, i.e., a preference for horizontal orientation.

To circumvent this issue, Bellot Rubio and Orozco Suárez ([2012](#)) analyzed data from the same instrument, recorded also at disk center, but averaged in time over 24 minutes. This allowed them to decrease the photon noise to $\sigma \approx 7 \times 10^{-5}$ such that almost 70 % of the internetwork displayed linear polarization signals clearly above the noise. The magnetic fields inferred from the analysis of these regions again showed a clear preference for the horizontal direction. However, the long integration times needed to decrease the noise might introduce additional effects (such as the cancellation of signals from opposite polarities and averaging over different structures) that need to be carefully addressed.

3.1.2 Preference for Vertical Fields

Ishikawa and Tsuneta ([2011](#)) studied, using also calibration curves, the very same data set as Orozco Suárez et al. ([2007](#)) and Lites et al. ([2008](#)). However, they concluded that the vertical magnetic field in the internetwork is almost as strong as the horizontal field. This would indicate a larger contribution from vertical (perpendicular to the solar surface) magnetic fields than in the aforementioned works. However, we note that the low value of the horizontal magnetic flux in Ishikawa and Tsuneta ([2011](#)) follows from their procedure to ascribe a zero value to the perpendicular component of the magnetic field whenever the linear polarization was deemed to be at, or below, the noise level ($B_\perp = 0$ if the line-integrated unsigned linear polarization $L_{\rm tot} \leq 1.5 \times 10^{-4}$). This approach has the problem of potentially deriving vertical magnetic fields from signals that are actually produced by strongly inclined fields. This happens because the most that can be said about signals with $L_{\rm tot} \leq 1.5 \times 10^{-4}$ is that $B_\perp$ is below some threshold value $B_{\rm thr,\perp}$. The problem is that if the value of this threshold is such that $B_{\rm thr} \gg B_\parallel$ then this approach will heavily underestimate the contribution of $B_\perp$ to the total magnetic field.

Mostly vertical fields have also been reported by Jafarzadeh et al. ([2014a](#)) using geometrical considerations in internetwork magnetic bright points seen at different photospheric layers. Unfortunately this method is not applicable to the majority of the internetwork (i.e., outside magnetic bright points).

---

[2]The noise level σ is given in units of the continuum intensity spatially averaged over the quiet Sun.

3.1.3 Isotropic and Quasi-isotropic Distribution

Asensio Ramos (2009) also analyzed spectropolarimetric data at disk center from Hinode (see Fig. 6), but applied a Bayesian technique to observations with a larger photon noise ($\sigma \approx 10^{-3}$) than all previously cited works. This resulted in an inferred angular distribution of the magnetic field in the internetwork that is close to isotropic. Asensio Ramos and Martínez González (2014) reached the same conclusion, although they could not exclude the existence of a non-negligible contribution from highly inclined magnetic fields.

An isotropic distribution was also favored by Martínez González et al. (2008). This work employed two spectral lines in the infrared (Fe I at 1565 nm) that are less affected by photon noise in the linear polarization, thus leading to more reliable inferences of $B_\perp$. Unlike most of the previous works, spectropolarimetric observations of the internetwork at various heliocentric viewing angles were considered. The resulting distribution of observed polarization signals (not of inferred magnetic fields) was found to be nearly independent of the viewing angle, suggesting an isotropic distribution of the IN fields. However, the authors emphasized that the observed distributions of polarimetric signals lacked a sufficiently large number of occurrences for signals above 4×10^{-3} (in units of the continuum intensity) to be considered statistically significant.

Borrero and Kobel (2013) also studied the distributions of polarimetric signals and tried to obtain more reliable statistics of spectropolarimetric observations at different heliocentric angles. To that end, they analysed a large data set from the Hinode satellite with a noise level of $\sigma \approx 3 \times 10^{-4}$. They found that the distribution of signals does in fact depend on the heliocentric angle, indicating a non-isotropic distribution of magnetic fields in the IN.

3.1.4 Bi-modal Distribution

The same data (see Fig. 6) as Asensio Ramos (2009) and Asensio Ramos and Martínez González (2014) was analyzed by Stenflo (2010), who employed a line-ratio technique aided by several calibration curves in order to disentangle thermodynamic and magnetic effects in the observed signals. He found evidence of two distinct populations of polarimetric signals in the internetwork. A population with a slope of the line-ratio[3] of $s \approx 1.15$ was attributed to strong (i.e. kilogauss) and mostly vertical magnetic fields, which remained unresolved at the spatial resolution of Hinode observations ($\approx 0.3''$). The second population of signals with a slope of $s \approx 1.66$ was ascribed to weak and isotropically distributed magnetic fields. These findings were further investigated by Steiner and Rezaei (2012), who analyzed polarimetric signals synthesized by solving the radiative transfer equation with input from three-dimensional MHD simulations. They also found the two populations with the same slopes as reported by Stenflo (2010). However, the two populations resulted from magnetic fields that, while all being weak, increase or decrease with height in the photosphere. Regardless of the physical realism of these simulations, the results by Steiner and Rezaei (2012) clearly point towards an uniqueness problem in the interpretation of the observed signals via the line-ratio technique.

3.1.5 Further Results

It has now become clear that data recorded at disk center are not sufficient to uniquely determine the angular distribution of the magnetic field in the internetwork. Indeed, the

---

[3]The line-ratio technique measures the ratio s of the amplitudes in the circular polarization signals in two different spectral lines. Under the assumption that both lines possess the same opacity and provided that the magnetic field is weak, then s is equal to the quotient of their Landé factors.

most recent attempts have focused on observations taken at several heliocentric angles, but a consensus has still not been reached. Using spectropolarimetric data from Hinode, Orozco Suárez and Katsukawa (2012) concluded that the distribution of the inclination of the magnetic field has a preference for the perpendicular direction (with respect to the line of sight) at all heliocentric angles studied ($\mu = 1.0, 0.5, 0.23, 0.1$). This result can be explained by magnetic fields that, being mostly horizontal at disk center, become gradually perpendicular to the solar surface for smaller μ values. We emphasize, however, that these results are possibly affected by the same bias as those of Orozco Suárez et al. (2007) (see Sect. 3.1.2). Borrero and Kobel (2013) also interpreted Hinode data in terms of IN magnetic fields that become gradually more horizontal for decreasing μ. This should not be considered a general trend because these authors employed only data at $\mu = 1.0$ and $\mu = 0.7$. In contrast, Stenflo (2013) concluded from spectropolarimetric observations of the Fe I lines at 525 nm taken with the ZIMPOL instrument that magnetic fields at $\mu = 0.5$ are more perpendicular to the solar surface (i.e., more vertical) than at $\mu = 0.1$.

Several effects can be invoked to explain why the angular distribution of IN magnetic fields changes with the heliocentric angle μ. For instance we could take into account that the height of formation of the spectral lines changes with μ because the continuum optical depth varies with the viewing angle: $\tau_c = f(\mu)$. This would readily introduce a μ-dependence in the angular distribution of IN magnetic fields if, as suggested by numerical simulations (Schüssler and Vögler 2008; Steiner et al. 2008; Steiner and Rezaei 2012; Rempel 2014), the angular distribution of the magnetic field changes with height in the photosphere. Alternatively, if τ_c is a slowly varying function of μ or if the angular distribution of the magnetic field does not vary with height on the photosphere, one could ascribe the μ-variations of the angular distribution to, for instance, an intrinsic difference between IN polar fields and those at the equator. In addition, it should be considered that the spatial resolution of the observations depends on μ, because, due to foreshortening, and given angular resolution element covers a larger piece of the solar surface near the limb than at disk centre. While in actuality all these effects are likely to play a role, it is not clear how to model them when interpreting the observations. A way to study which of the first two aforementioned effects is more important would be by means of high signal-to-noise spectropolarimetric observations along the equator and along the central meridian.

3.1.6 Future Prospects

In spite of many efforts, we are currently no closer to accurately determining the angular distribution of the magnetic field in the internetwork than we were a decade ago. This results from a combination of the effects of photon noise and signal selection, as well as from the different techniques employed to infer the magnetic field from spectropolarimetric signals produced by the Zeeman effect. Advances on this front could be achieved by means of spectropolarimetric observations in the infrared. In particular, the Fe I line pair at 1565 nm is much less affected by noise in the linear polarization (see Sect. 3.1.3). Moreover, the continuum of these spectral lines is formed deeper (about 70–100 km deeper depending on the opacity sources included in the calculation of the absorption coefficient) than in the commonly used Fe I line pair at 630 nm. Therefore, these spectral lines are best suited to study the angular distribution of the magnetic field in the lower layers of the photosphere (see Sect. 3.1). The only drawback comes from the lower spatial resolution in the infrared, but this will be alleviated in the near future with observations using large-aperture telescopes such as GREGOR and DKIST, thanks to their large primary mirrors and hence smaller diffraction limits. The former one, with a 1.5-meter aperture, is already obtaining

spectropolarimetric observations in these spectral lines with a spatial resolution comparable to that of the Hinode telescope in the visible (Collados et al. 2012).

Spectral lines whose spectropolarimetric signals are produced by the Hanle effect are also worth considering for future observations and analysis. Indeed, in the saturated Hanle regime the linear polarization signals depend only on the orientation of the magnetic field, but not on its magnitude (Carlin and Asensio Ramos 2015). This removes an important source of uncertainty. In addition, Hanle signals are less affected by cancellation effects if the magnetic field is unresolved. This feature of the Hanle effect is particularly relevant for investigations of the magnetic field produced by a small-scale turbulent dynamo. It remains to be seen, however, how accurately our theoretical understanding of the Hanle effect and its intricate interactions with the thermodynamics and kinematics of the plasma (Carlin et al. 2012) allow us to determine the properties of IN magnetic fields.

3.2 Solar Cycle Variations

The presence of a small-scale turbulent dynamo that operates independently of the large-scale dynamo responsible for the 11-year activity cycle would provide a time-independent background level of unsigned magnetic flux in the quiet Sun.

From ground-based observations Sánchez Almeida (2003) concluded that there is no correlation between the strength of the magnetic field in the internetwork and the solar cycle. However, to study this particular aspect of the magnetic fields in the internetwork, it is necessary to employ high-quality long-term observations of the polarization signals in spectral lines. This is the case for the synoptic observations carried out by Hinode's spectropolarimeter. Bühler et al. (2013); Jin and Wang (2015a, 2015b) analysed these data and concluded that during the period between 2006–2015 the magnetic field in IN regions at disk center did not vary significantly. This result was later extended by Lites et al. (2014) (see Fig. 7) to cover both low and mid latitudes ($\mu \geq 0.5$). While these studies were based on the Zeeman effect in Fe I lines at 630 nm, Kleint et al. (2010) and Bianda et al. (2014) analysed spectropolarimetric data from the ZIMPOL instrument in the Sr I line at 460 nm and in molecular C_2 lines at 514 nm. The polarization signals of the recorded spectral lines are produced by the Hanle effect, which is much less affected by cancellation than the Zeeman effect for magnetic fields of opposite polarities. These authors concluded that for the period between 2007 to 2009 (solar minimum) the magnetic field strength in the IN remained the same. However, they report a possible variation with respect to earlier measurements obtained in 2000 (solar maximum).

3.3 Small-Scale Events

While most polarimetric signals in the internetwork are at or below the noise level of the observations (Sect. 3.1), some features show particularly strong signals. Detailed analysis of these revealed a variety of dynamic magnetic phenomena taking place in the internetwork. This is not surprising because the magnetic field in the internetwork is not strong enough to dominate over convective motions. Instead, these motions twist and bend the field lines into complicated patterns. This leads to large variations of the magnetic, kinematic and thermodynamic properties on small scales, which manifest themselves in complex spectropolarimetric signals featuring large asymmetries and additional components or lobes.

Since the observational signals associated with such small-scale phenomena are very dynamic and short-lived, high-cadence instruments attached to seeing-free telescopes (Hinode, Sunrise) or large-aperture telescopes at the ground (SST, GREGOR), are required to characterize them. In the following we summarize some of the recent results.
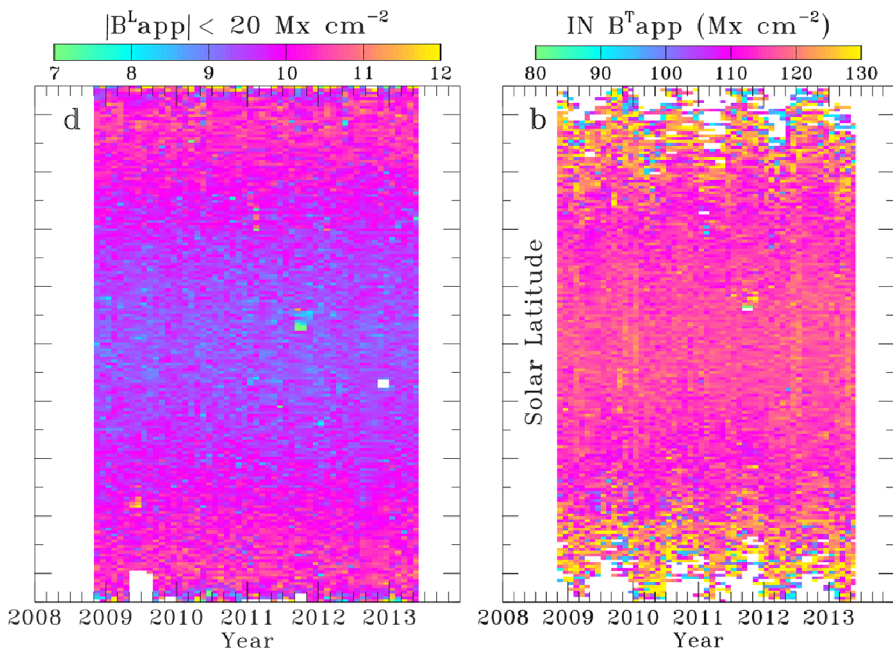
Fig. 7 Unsigned longitudinal component (*left panel*) and transversal component (*right panel*) of the magnetic field in the internetwork as a function of time (*abcissa*) and solar latitude (*ordinate*, from $-90°$ to $+90°$ with tickmarks at intervals of $10°$). The time coverage spans from 2009 (close to solar minimum) until 2013 (close to solar maximum). Figure adapted from Lites et al. (2014), reproduced with permissions from the Oxford University Press on behalf of the Astronomical Society of Japan

3.3.1 Emergence of Magnetic Loops

The emergence of magnetic Ω-loops has been studied in detail, by Centeno et al. (2007) and Martínez González and Bellot Rubio (2009) using Hinode data. Such loops are observed as single patches of linear polarization (indicating horizontal magnetic fields) that are seen prior to the appearance of two patches of opposite circular polarization (indicating magnetic fields of opposite polarities) at the endpoints of the elongated horizontal field patch. As it evolves in time, the horizontal magnetic field disappears and the footpoints of opposite polarities separate. While these observations are, in principle, compatible with both an emerging Ω-loop and a submerging inverted Ω-loop, the former interpretation is preferred whenever the initial horizontal field usually is found in upflow regions (i.e., granules). Those appearing in downflow regions are therefore associated to inverted Ω-loops (Pietarila et al. 2011).

The lifetime of a few minutes and size of 1–2″ of the features are very similar to corresponding quantities of granules. From observations of the Mg I 517 nm and Ca II 396 nm spectral lines (formed in the mid and lower chromosphere, respectively) (Martínez González et al. 2010) concluded that many of the loops reach the lower chromosphere, carrying magnetic energy at a rate of $\approx 2 \times 10^6$ erg cm^{-2} s^{-1}.

However, not all horizontal fields observed in the internetwork are part of an emergence process. Danilovic et al. (2010a) analysed spectropolarimetric observations of the Fe I line at 525 nm with the IMaX instrument on-board Sunrise. They studied a large number of internetwork horizontal field patches and concluded that, although they tend to appear at
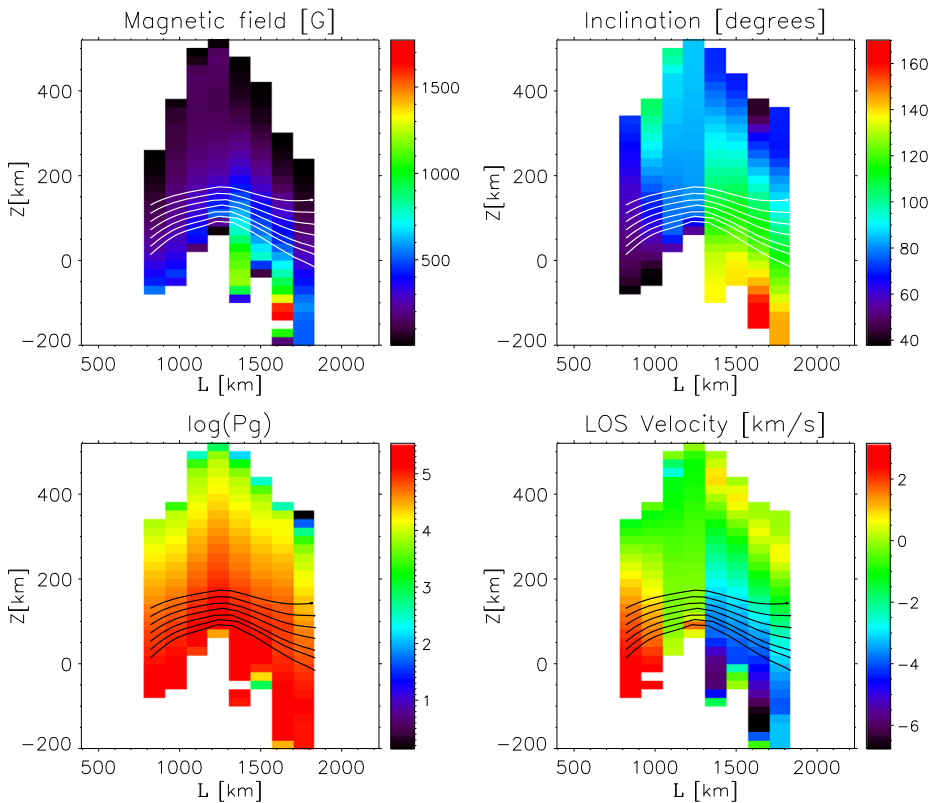
Fig. 8 Side-view of a magnetic Ω-loop seen in Hinode/SP data (Quintero Noda et al. 2014): magnetic field strength (*upper-left*), magnetic field inclination with respect to the vertical direction (*upper-right*), gas pressure (*lower-left*), line-of-sight velocity (*lower-right*). The magnetic field at the *left* and *right* footpoints of the loop points upwards and downwards, respectively. On the other hand, the velocity points *downwards* and *upwards* at the *left* and *right* footpoints, respectively, with the latter reaching values up to $-6\,\mathrm{km\,s^{-1}}$ (supersonic). Reproduced with permission from Astronomy & Astrophysics, ©ESO

the boundary of granules, most of them are caught at some point in their evolution in an intergranular lane. This makes it difficult to uniquely ascribe them to a emergence of submergence event. These authors also found that horizontal IN fields do not possess a typical life-time or size.

3.3.2 Siphon-Flows Along Magnetic Loops

Highly asymmetric, single-lobed Stokes *V* profiles are often observed at the footpoints of the magnetic loops discussed in the previous subsection (Sainz Dalda et al. 2012). Viticchié (2012) interpreted them as being produced by a siphon flow along the magnetic loop (Meyer and Schmidt 1968a, 1968b). This conclusion is supported by Quintero Noda et al. (2014), who also found that the flow has the opposite direction at the two footpoints and can become supersonic in between (see Fig. 8). Supersonic siphon flows had been theoretically predicted by Thomas and Montesinos (1990) and already observationally detected by Rüedi et al. (1992a) and Degenhardt et al. (1993).

3.3.3 Supersonic Upflows

Borrero et al. (2010) found highly blue-shifted Stokes V signals in Sunrise/IMaX data, appearing close to, but not exactly at, locations with large linear polarization signals (i.e., horizontal magnetic fields). They ascribed these signals to supersonic magnetic upflows occurring at the centers or edges of granules. According to Quintero Noda et al. (2013) the detection of the linear polarization signal precedes the neighbouring supersonic upflow (highly blue-shifted circular polarization). Rubio da Costa et al. (2015) studied many such events at different positions on the solar disk and found that their properties do not vary significantly with the heliocentric angle.

Borrero et al. (2013) suggested that the supersonic upflows were caused by the reconnection of an emerging Ω-loop with an ambient field of opposite polarity (Parker 1972, 1973). However, this particular interpretation has been questioned by Danilovic et al. (2015) who, analyzing synthetic spectropolarimetric data obtained from MHD simulations, found that the same observational features can also be reproduced in the absence of reconnection. Instead they propose a magnetic topology that closely resembles that of a plasma bubble filled with a strong unipolar magnetic field that rises through the photosphere. Structures with very similar magnetic topologies but moving downwards had previously been reported by Quintero Noda et al. (2014).

3.3.4 Magnetic Elements in the Internetwork

Magnetic flux concentrations sufficiently large to appear in the form of bright points are also present in the internetwork but, unlike in the network, they appear isolated and are less abundant: 2.2 bright points per Mm^2 in the network versus 0.85 in the internetwork (Sánchez Almeida et al. 2010). Note that, in addition, smaller kG flux concentrations may exist that are not resolved by the observations.

The properties of the internetwork elements are rather diverse. Some of them are observed as mostly horizontal fields with a lifetime of 1–10 minutes and typical sizes of several arcseconds. These *transient horizontal fields* (THFs) were previously detected in plage regions and extensively studied by Ishikawa et al. (2008) using Hinode data. Later, Ishikawa and Tsuneta (2009) found that THFs in in plages feature very similar distributions for the vertical and horizontal component of the magnetic field (after removing the bias caused by persistent vertical fields in the plage) than those in the internetwork. Additionally they found that, whereas THFs in plage regions are preferentially oriented along the plage's direction, internetwork THFs possess no preferred orientation. This indicates that the topology of THFs magnetic field in plages depends on the large scale structure of the surrounding field and their formation might be associated with the emergence of magnetic flux in the Photosphere. A detailed investigation of the magnetic topology in THFs was later carried out by Ishikawa et al. (2010), who found that they correspond to emerging Ω-loops similar to those described in Sect. 3.3.1.

Other isolated internetwork magnetic elements are seen mostly in the circular polarization, thus indicating the presence of mostly vertical and strong (kGs) magnetic fields. Using Sunrise/IMaX data (Martínez González et al. 2011b) discovered damped oscillations in the magnetic flux of some of these elements.

Internetwork magnetic elements have been found to migrate towards the surrounding network boundaries (de Wijn et al. 2008), being advected by supergranular flows (Orozco Suárez et al. 2012). Using Hinode/SP data Utz et al. (2010) and Manso Sainz et al. (2011) discovered that, during this migration process, the magnetic elements behave as random

walkers. High spatial-resolution observations from SST, BBSO, and Sunrise revealed, however, super-diffusive trajectories for the internetwork magnetic bright points (Abramenko et al. 2011; Chitta et al. 2012; Jafarzadeh et al. 2014b). The latter study showed that their horizontal motion could be described as a random walker (due to turbulence in intergranular lanes and granular evolution) superposed on a systematic velocity (caused by granular, meso-, and super-granular flows). That analysis also revealed that the diffusion coefficients of the motion of the internetwork magnetic bright points lie within the range obtained from the decay rates of the magnetic field on the solar surface in 3D radiative MHD simulations of Cameron et al. (2011).

4 Small-Scale Dynamo

As discussed in detail in Sect. 3, observations indicate the existence of an ubiquitous small-scale "turbulent" magnetic field, which apparently does not vary in the course of the solar cycle. Petrovay and Szakaly (1993) were the first to suggest that such a field would be generated by a small-scale dynamo (SSD), which is independent of the large-scale dynamo (LSD) responsible for the global (system-scale) magnetic field of the solar cycle. For the LSD (for a review, see Charbonneau 2010), differential rotation and the Coriolis force are essential ingredients, leading to large-scale poloidal and toroidal magnetic fields. In contrast, the SSD generates a magnetic field also in the absence of rotation through stretching, twisting and folding of field lines by a flow with chaotic streamlines (such as turbulence), if the magnetic Reynolds number of the flow is high enough. The generated field is of mixed polarity on spatial scales small compared to the integral scale of the flow and its large-scale average vanishes. Therefore, the SSD is sometimes also denominated as "fluctuation dynamo". In the solar literature, the term "local dynamo" has also been used occasionally. This is potentially misleading if understood as a locality in space, e.g., in the granulation layer: SSD action probably takes place throughout the whole convection zone (Hotta et al. 2015), modified by rotational shear and Coriolis force in the deeper layers. The SSD is also not local in wavelength space since the large-scale convective patterns imprint themselves on the distribution of the SSD-generated field by flux transport and expulsion, leading to a flat spectrum at large scales for the saturated dynamo state (Rempel 2014).

First suggestions of a turbulent SSD dynamo go back to Batchelor (1950), who drew on the analogy between the hydrodynamic vorticity equation and the magnetic induction equation in the kinematic limit. For an idealized case, SSD action was first demonstrated by Kazantsev (1968). Starting with Meneguzzi et al. (1981), the operation of SSDs was later found in many simulations of forced turbulence as well as for incompressible, Boussinesq, and anelastic thermal convection (for reviews, see Brandenburg and Subramanian 2005; Brandenburg et al. 2012; Tobias et al. 2013). Most of these simulations were carried out for fluids with magnetic Prandtl number $P_M = \nu/\eta$ (ν: kinematic viscosity, η: magnetic diffusivity) of order unity or bigger. The regime $P_M \ll 1$, which is relevant for the Sun ($P_M \approx 10^{-5}$), is much more demanding computationally and thus not well covered by simulations. Heuristic arguments suggest that a SSD is more difficult to excite (i.e., requires higher magnetic Reynolds number) for low Prandtl number and it was debated for some time whether SSD action is possible at all in this regime. Several studies showed, however, that the critical magnetic Reynolds number increases only moderately for $P_M \ll 1$ (Brandenburg 2011; Buchlin 2011; Tobias et al. 2013). Therefore, SSD action is expected for solar conditions, owing to the high magnetic Reynolds numbers of solar convection.

Direct simulations of SSD action under solar conditions is computationally unfeasible owing to the extreme values of the (kinetic and magnetic) Reynolds numbers and of P_M in the convection zone. For comprehensive simulations representing the relevant physical processes in the upper solar convection zone and photosphere (compressible convection, partial ionization, proper radiative energy transport), one has therefore to resort to large-eddy simulations: artificial diffusivities are introduced such that they minimize diffusion on the numerically resolved scales and provide an efficient diffusive cutoff at the grid scale (cf. Rempel et al. 2009; Rempel 2014; Miesch et al. 2015). It can be argued that these procedures lead to effective magnetic Prandtl numbers of order unity. It is not clear, therefore, that such simulations correctly represent the putative SSD action on the Sun. On the other hand, simulations of convection, of magneto-convection with an imposed background field, as well as of sunspots are consistent with observations on all spatial scales reached by the latter (e.g., Nordlund et al. 2009; Stein 2012; Rempel and Schlichenmaier 2011). Furthermore, it is well conceivable that saturated SSD action reaches a saturated state for which all flow scales smaller than the resistive cutoff are suppressed by the Lorentz force, leading to an effective magnetic Prandtl number of order unity. In any case, comprehensive simulations provide self-consistent data for the forward modelling of observations and test cases for data analysis methods.

Comprehensive simulations carried out so far suggest that SSD action is indeed pervasive in the convection zone (Vögler and Schüssler 2007; Pietarila Graham et al. 2010; Rempel 2014; Hotta et al. 2015), at least for effective magnetic Prandtl numbers of order unity (Thaler and Spruit 2015). The structure of the generated magnetic field is in many regards similar to the turbulent internetwork field inferred from observations (Schüssler and Vögler 2008; Pietarila Graham et al. 2009; Danilovic et al. 2010b; Schüssler 2013). The amplitude of the simulated field, however, appears to fall short of the observational inferences (Danilovic et al. 2010a; Shchukina and Trujillo Bueno 2011), unless the lower boundary condition is modified (Rempel 2014, discussed further below).

Figure 9 shows a snapshot from a near-surface SSD simulation with the MURaM code. The computational box had a size of 18×18 Mm^2 horizontally and 7 Mm vertically, reaching about 1 Mm above the optical surface (average height of bolometric optical depth unity). The run was started from a relaxed hydrodynamic run with a 4×4 checkerboard sinusoidal seed field of 0.1 G amplitude. The run was then continued with stepwise increases of the grid resolution, for 10.4 hours of solar time, thus achieving a statistically stationary state. Within the full box, the saturated rms field strength was 488 G and the average unsigned vertical field at optical depth unity reached 19.4 G. The magnetic field exhibits the typical 'salt-and-pepper' structure of SSD action with mixed polarity at small scales, resulting from turbulent eddies providing the 'stretch-twist-fold' mechanism for flux generation (Zeldovich et al. 1983). This is also reflected in the fact that the magnetic flux is found predominantly at those locations where the velocity appears 'rough', indicating enhanced turbulence. Most of the complexity of the SSD-generated field is lost, however, when observed with limited spatial resolution. The lower left panel of Fig. 9 shows the result of convolving the upper-right field map with an Airy function corresponding to a 50-cm telescope (such as the one onboard Hinode) at a wavelength of 630 nm. When watching a time evolution of such maps, one detects many instances of the apparent emergence or cancellation of bipoles, but these events mostly result from the smoothing over much a more complex magnetic structure.

Spatial smoothing and the resulting cancellation of opposite-polarity fields has also drastic effects on the unsigned flux (average unsigned vertical field component, $\langle |B_z| \rangle$) detectable at a given spatial resolution. At the original grid resolution of the simulation discussed here, we have $\langle |B_z| \rangle = 19.4$ G at optical depth unity. Smoothing with Airy functions
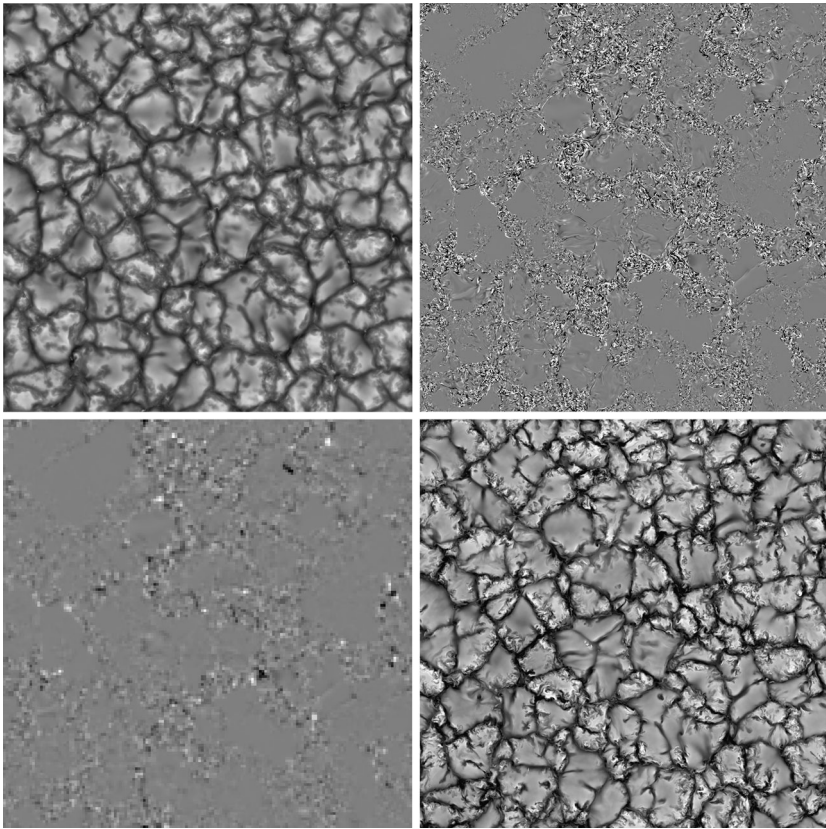
Fig. 9 Snapshot from a SSD simulation with the MURaM code. Shown are maps of the bolometric intensity (*upper left*), the vertical magnetic field component at optical depth unity at simulation resolution (*upper right*) and smoothed with an Airy function corresponding to a 50-cm telescope at 630 nm (*lower left*), both saturated at ± 100 G, and the vertical velocity component at optical depth unity (*lower right*); upflows are represented by *brighter*, downflows by *darker shades*, saturated at ± 5 km s^{-1}. The size of the computational box is 18×18 Mm^2 horizontally and 7 Mm in depth, with a grid cell size of 10 km

corresponding to spatial resolutions of 0.1″, 0.2″, and 1″ leads to values of 9 G, 5.3 G, and 1.1 G, respectively. These are actually upper limits since the effects of a realistic MTF and noise would significantly decrease the values of $\langle |B_z| \rangle$ even further. On the other hand, this simulation probably underestimates the unsigned flux by about a factor 3 (see discussion further below).

The overall spatial distribution of the magnetic field reflects the scales of the convective flows. The magnetic structures are transported towards the downflow regions, where they accumulate and outline the convective flow patterns from the dominant granulation scale up to the largest flow scale in this simulation of about 6 Mm, which is determined by the depth of the computational box. As a result, the flux distribution is spatially inhomogeneous at these scales and flux-deficient 'voids' appear in the distribution of the magnetic field (Martínez González et al. 2012a). In the simulation, their size is limited by the depth of the box, but in the real Sun the maximum size of the voids is reached when the time scale of the flow pattern becomes about equal to the growth time of the SSD in the near surface layers. As the simulations show, the formation of voids is not in contradiction to the generation of mag-
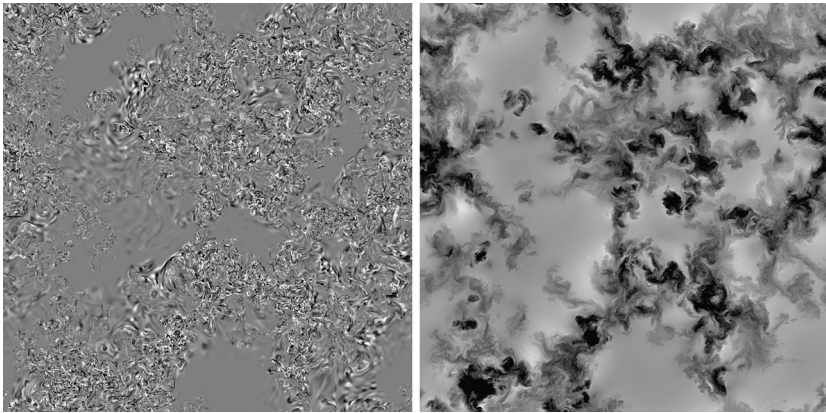
Fig. 10 Vertical components of magnetic field (*left*) and velocity (*right*) in a depth of 5 Mm below the optical surface for the same snapshot as shown in Fig. 9. The greyscales are saturated for ± 1800 G and ± 1.2 km s^{-1}, respectively. Upflows are represented by *brighter*, downflows by *darker shades*

Fig. 11 Ratio of actual field strength and equipartition field strength with respect to the kinetic energy density of the convective flows (both horizontally averaged) as a function of height for the same snapshot as shown in Figs. 9 and 10. $z = 0$ refers to the optical surface
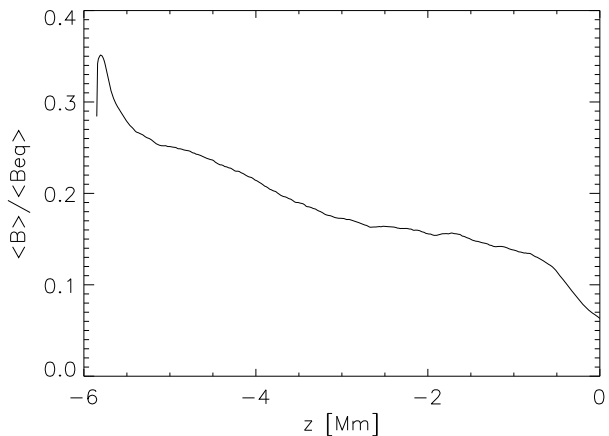
netic flux mainly in the turbulent intergranular lanes (cf. Martínez Pillet 2013): the lanes are advected by the larger-scale flows while the field is amplified by the SSD. The voids would be there even if the operation of the SSD were limited to the near-surface granulation layer in the sense of a truly 'local dynamo'. However, this is not the case: the simulations show that SSD action involves the whole convecting volume and in global simulations pervades the whole convection zone (Hotta et al. 2015).

Figure 10 shows maps of the vertical field and vertical velocity in the deeper layers of the box, at a depth of 5 Mm. The salt-and-pepper structure of the magnetic field and its association with the downflow patterns (dark in the greyscale representation) is similar to the near-surface maps shown in Fig. 9. Also the 'voids', which appear at roughly the same positions as near the surface, are clearly associated with the upflow regions of the larger-scale convective pattern at that depth.

The field strength divided by the equipartition field strength (with respect to the kinetic energy density of the convective flows) given in Fig. 11 increases with depth and shows that the SSD is rather efficient, even though the layers below the simulation box are (unrealis-
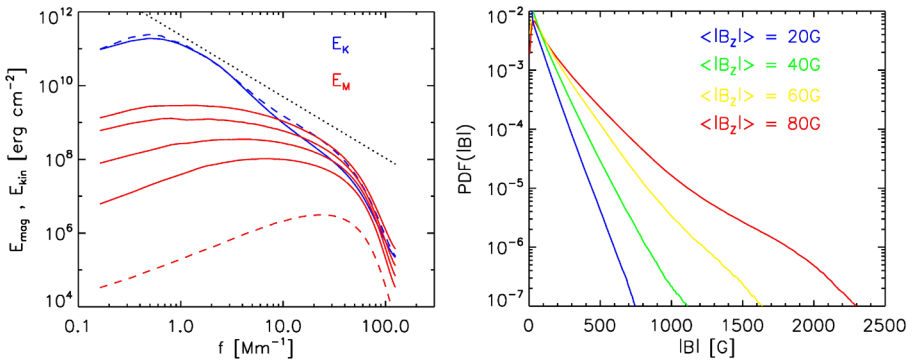
Fig. 12 *Left panel*: kinetic energy spectra (*blue curves*) and magnetic energy spectra (*red curves*, at different times during the growth phase of the dynamo, corresponding to the levels of the mean magnetic field strength indicated in the *right panel*) at the optical surface for a SSD run. *Dashed lines* indicate the kinematic phase (scaled up for the magnetic energy in order to show it on the same plot). The *full blue curve* and the *uppermost red curve* correspond to the saturated state of the dynamo. The *dotted line* indicates a slope of $-5/3$. *Right panel*: field strength distribution (PDFs) at the optical surface for various levels of the mean vertical field during the growth phase of the dynamo (from Rempel 2014, Fig. 2; ©AAS, reproduced with permission)

tically) assumed to be field-free. In total, the magnetic energy amounts to about 7.4 % of the kinetic energy in the box. In the global simulations of Hotta et al. (2015), the magnetic energy density reaches 95 % of the equipartition value near the bottom of the convection zone, with a significant suppression of the convective flow velocities due to the action of the Lorentz force. This shows that SSD action is much more efficient than the large-scale dynamo in converting kinetic to magnetic energy.

When synthetic Stokes profiles are calculated from simulations and compared with observations of the internetwork or turbulent fields (e.g., Danilovic et al. 2010a; Shchukina and Trujillo Bueno 2011), SSD simulations in shallow boxes without advection of magnetic flux from below (such as the example presented above) appear to provide too little unsigned flux. Typical values for $\langle |B_z| \rangle$ at the optical surface are 20–30 G while the observations require at least a factor 3 more magnetic flux. This may partly be due to too low values of the magnetic Reynolds number, although this may affect the saturated state much less than the kinematic growth rate (see below).

Another reason for too low surface flux from the SSD results from the lower boundary condition. In order to demonstrate proper SSD action in the simulation box, the simulations of Vögler and Schüssler (2007) and Pietarila Graham et al. (2010) did not allow the advection of magnetic flux by upflows (inflows) at the lower boundary; only flux transport out of the box was permitted. Therefore, the deeper layers of the convection zone were implicitly assumed to be field free and SSD action was artificially restricted to the volume of the box. This is not expected to be the case in the real Sun, where flux generated by SSD action in the deeper layers probably contributes to the surface field as well. In this sense, a more realistic boundary condition is symmetric for magnetic field, i.e., assuming that the internal magnetic structure continues smoothly to the deeper levels. This implies that inflows now can transport magnetic flux into the box, so that we no longer have dynamo action in a strict sense (i.e., no external sources) in such simulations, which nevertheless are probably more realistic.

Simulations with a symmetric lower boundary condition for the magnetic field have been carried out recently by Rempel (2014, hereafter referred to as R14). He tested the effect of the boundary condition by comparing two simulations with different depths of the bottom
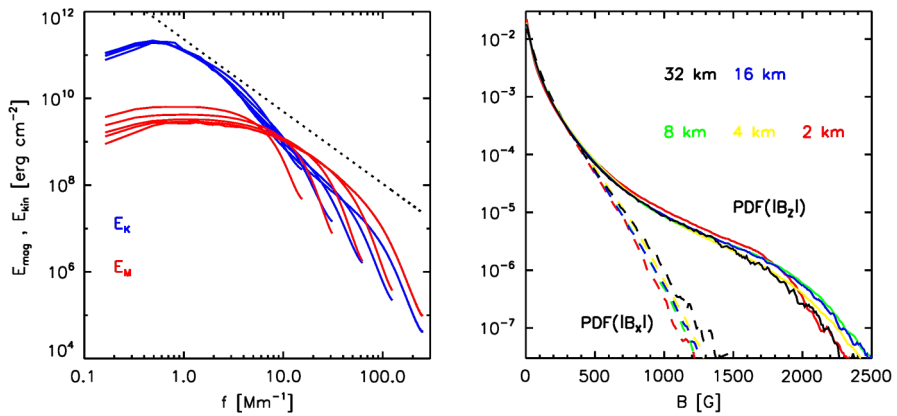
Fig. 13 Dependence on grid resolution. *Left panel*: spectra of magnetic (*red*) and kinetic (*blue*) energy. The *dotted line* indicates the Kolmogorov scaling (slope $-5/3$). *Right panel*: PDFs of the vertical field (B_z) and of one component of the horizontal field (B_x). The result for the other horizontal component is almost identical. Grid resolution varies from 32 km to 2 km (adapted from Rempel 2014, Fig. 3; ©AAS, reproduced with permission)

(2.2 Mm and 7 Mm, respectively). It turned out that the average magnetic quantities in the shallow box agreed quite well with those in the corresponding part of the deep box. This means that the symmetric boundary condition does a fairly good job in representing SSD action below the box. A simulation with a grid spacing of 4 km in a box of 6.1×6.1 Mm^2 horizontal size and 3.1 Mm depth provides $\langle |B_z| \rangle = 86$ G at the optical surface for the saturated state, an amplitude that is compatible with spectro-polarimetric observations. The magnetic structure is still of mixed polarity on small scales, with more sheet-like structures in the intergranular lanes (see Fig. 1 of R14). Figure 12 shows the time evolution of the magnetic and kinetic energy spectra and of the field strength distribution (probability density function, PDF) at the optical surface for this run, which started with a random seed field of 10^{-3} G inserted in a relaxed hydrodynamic simulation. Dashed lines indicate the early kinematic state, for which the magnetic energy peaks near the diffusive cutoff. As time progresses, the maximum moves towards larger scales and the spectrum becomes nearly flat for low wave numbers in the saturated state. This should not be misinterpreted as indicating that a large-scale component (in the sense of a mean field) develops: it just represents the organization (by flux expulsion) of the small-scale field in the patterns of convective flows, which cover all scales from granulation up to the depth of the box. In the saturated state, the Lorentz force feedback leads to a suppression of the kinetic energy on scales below 100 km. The PDFs (right panel of Fig. 12) show a growing fraction of kG fields; they correspond to intergranular flux concentrations covering about 0.5 % of the area at the optical surface, often appearing as bright points in continuum images (cf. Fig. 15). The density of such bright points in the quiet Sun can be taken as an observational measure of the amplitude of SSD action, i.e. the mean unsigned vertical field (Sánchez Almeida et al. 2010).

The dependence of the SSD results on grid resolution for the same simulation setup is shown in Fig. 13. The quasi-stationary saturated regime was reached in all cases. For increasing grid resolution, the energy spectra converge at larger scales while the small-scale part becomes more extended. As far as the large scales are concerned, the simulation has converged for a grid resolution of 8 km. The magnetic energy exceeds the kinetic energy at small scales by about a factor 2, a result also found in direct SSD simulations, i.e., simulations with physical diffusion terms (Brandenburg and Subramanian 2005). The PDFs (right
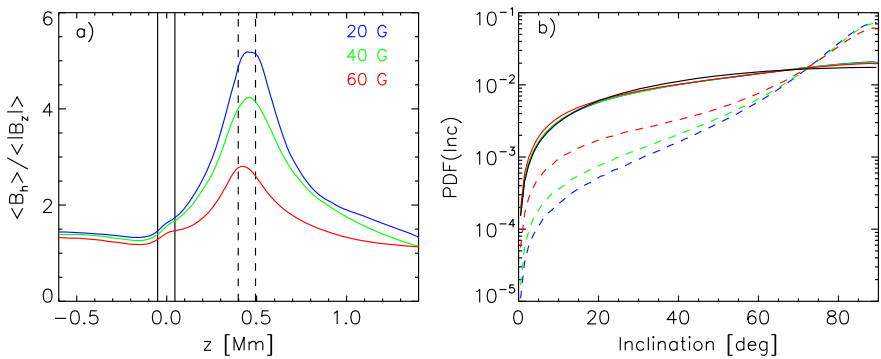
Fig. 14 Angular distribution of the field vector. Panel (**a**) gives the ratio of horizontal to vertical field strength, both horizontally averaged, as a function of height ($z = 0$ refers to the optical surface). The *line colors* correspond to simulations with different mean flux density of the vertical field at $z = 0$. (**b**) Probability distribution functions of the field inclination (with respect to the vertical direction) for two different layers indicated by *vertical lines* in panel (**a**). *Full lines* refer to a layer near the visible surface, *dashed lines* to a height around 450 km. The *black solid line* indicates a perfectly isotropic distribution (from Rempel 2014, Fig. 14; ©AAS, reproduced with permission)

panel of Fig. 13) do not change significantly with increasing grid resolution. These results indicate that, at least in the framework of the numerical approach taken, the simulation results reach an asymptotic limit on scales above about 50 km. Increasing resolution only smoothly extends the spectra to smaller scales.

In an unstratified medium without a preferred direction, the orientations of the magnetic field generated by a SSD are isotropically distributed. This is also to be expected in a stratified medium as long as scales smaller than the pressure scale height are considered. SSD simulations under solar conditions in fact exhibit isotropic field distributions in the subsurface layers, but show a strong preference for horizontal fields in the middle photosphere (Schüssler and Vögler 2008; Rempel 2014). This would be in accordance with some observational inferences (e.g., Harvey et al. 2007; Lites et al. 2008; Orozco Suárez and Katsukawa 2012, see the detailed discussion in Sect. 3.1). Figure 14 illustrates this result on the basis of the SSD simulations of Rempel (2014). The ratio of the horizontally averaged horizontal and vertical field components (left panel) changes from values consistent with an isotropic distribution at the optical surface and below to a strong dominance of horizontal fields in a layer centered at about 450 km height in the photosphere. The preference for horizontal field is less pronounced for higher mean vertical flux densities. The right panel of Fig. 14 gives probability distribution functions of the field orientation for two layers: around the optical surface (full lines) and between 450 km and 500 km (dashed lines). The distributions are nearly isotropic in the lower layer, but dominated by inclined fields in the upper layer. Two physical mechanisms have been suggested to contribute to the dominance of horizontal fields in the middle photosphere: (1) since the SSD-generated field is of mixed polarity on small scales, the magnetic loops connecting nearby opposite-polarity patches reach maximal heights comparable to their footpoint separations (Schüssler and Vögler 2008), and (2) by flux expulsion, the overturning flows of granular convection concentrate the horizontal field in the middle photosphere (Steiner et al. 2008; Steiner and Rezaei 2012).

Figure 15 shows a comparison of SSD simulations in a small, shallow box ($6.1 \times 6.1 \times 3.1$ Mm^3) and in a big, deep box ($24.6 \times 24.6 \times 7.7$ Mm^3), both at a grid resolution of 16 km. The figure shows maps of the bolometric brightness (left panel) and the vertical magnetic
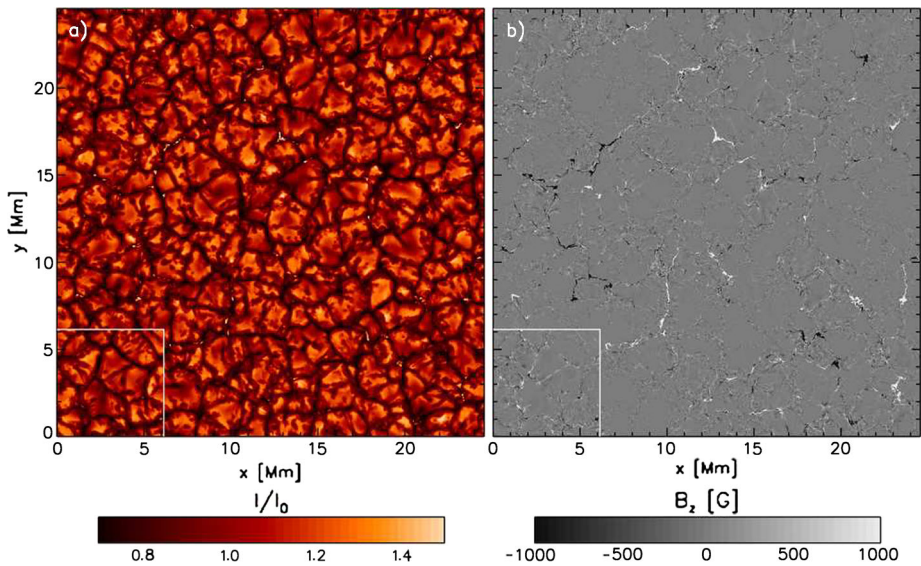
Fig. 15 Maps of bolometric intensity (*left*) and vertical magnetic field at the optical surface (*right*) for a SSD simulation in a big and 7.7 Mm deep box, compared to the result of a simulation in a smaller of 3.1 Mm depth (inserted at the *lower left corner* of the maps). The larger-scale convective flow patterns in the big box lead to a network-like structure of the field with bigger patches of positive and negative flux appearing as bright structures (from Rempel 2014, Fig. 14; ©AAS, reproduced with permission)

field component at the optical surface (right panel). A snapshot from the simulation in the small, shallow box is inserted at the lower left corner of both maps. In the big box, a network structure of the magnetic flux on a scale of 5–10 Mm has developed, which is a result of flux advection by convective flows on the corresponding spatial scales. Larger patches of concentrated magnetic flux appear as bright structures in the intensity image. These are absent in the simulation in the small box, where the responsible longer-lived, larger-scale flows cannot develop. The energy spectra of both simulations differ only in their extension towards larger scales. The PDFs of the vertical magnetic field shows a pronounced strong-field bump in the case of the big box, while those of the horizontal field do not significantly differ. The two simulations are also consistent with each other in terms of the depth-dependence of horizontally averaged RMS field strength, indicating that the symmetric magnetic boundary condition provides a reasonable representation of the SSD field below the simulation box (Figs. 9 and 10 in Rempel 2014, not shown here).

5 Concluding Remarks and Outlook

Although the heliographic distribution of plage and network magnetic fields is rather different, as is the source of these fields, the properties of the individual magnetic features therein are relatively similar, suggesting that their properties are determined mainly by local effects (such as the efficiency of the flux expulsion and convective collapse processes) rather than global parameters. The largest advances in recent years in attaining knowledge and an understanding of the structure of and the processes acting within plage and network magnetic elements have been driven by high resolution observations and by 3D MHD simulations.

Thus the combination of high-resolution observations and MHD simulations suggests that the simple classical description of these flux concentrations in terms of thin flux tubes still holds for many purposes, although additional features are being uncovered, such as return-flux in the surroundings of the flux concentrations or the fact that the kG fields within the magnetic features are not in all cases long-lived. As the spatial resolution of observations continues to increase and simulations become ever more sophisticated, we expect to obtain further insights into these magnetic features. In particular, the role played by a small-scale dynamo in feeding the plage and network fields is open and promises to become an exciting field of research.

The lack of sufficient spatial resolution and the insufficient signal-to-noise ratio of spectropolarimetric observations still limit our capability to correctly determine the properties of internetwork magnetic fields. This has been aggravated by the use of analysis methods that are biased towards certain sorts of distributions. While better observations will certainly help, attention must also be paid to data recorded at different heliocentric positions and in spectral lines formed at different heights, as well as in lines whose polarization signals are produced by mechanisms other than the Zeeman effect. Last but not least, we must continue to make use of forward analysis employing known distributions of magnetic fields, be it by means of simple analytical distributions or by means of more complex (i.e., realistic) distributions from MHD simulations, in order to understand the various biases and uncertainties introduced by noise, analysis technique, center-to-limb effects, and so forth. Although some of these needs will be met in the near future with the arrival of new space missions and large-aperture telescopes, the remaining ones still require further and detailed investigations.

Small-scale dynamo action is a plausible candidate for the source of the observed internetwork and 'turbulent' fields. It may contribute to the flux supply of network fields and it may affect the operation of the large-scale dynamo (Cattaneo and Tobias 2014; Squire and Bhattacharjee 2015). Small-scale dynamo action is found in near-surface local-box simulations and in global spherical simulations. Although their results are consistent with a number of observed properties of the internetwork field, the simulations are carried for (effective) Reynolds numbers and magnetic Prandtl numbers that are far from the regime in which the Sun operates. Nonlinear effects, i.e., the suppression of small-scale motions by the generated magnetic field might alleviate this problem. This point needs to be clarified also by direct numerical simulations (using explicit diffusivities) with a sufficiently high resolution so that magnetic Prandtl numbers significantly below unity can be reached. As observations of the internetwork field grow more sensitive and better resolved with the new telescopes and innovative polarimetric instrumentation that are now becoming available, a much more detailed comparison between observation and simulation will be possible. This will certainly put the realism of the solar small-scale dynamo simulations to a critical test. This is the more important since the small-scale dynamo is a rather fundamental hydromagnetic process, which has potential implications for a considerable number of astrophysical systems. The combination of solar observations and simulations so far provide the only possibility to study this process in a natural environment.

References

V.I. Abramenko, D.W. Longcope, Distribution of the magnetic flux in elements of the magnetic field in active regions. Astrophys. J. **619**, 1160–1166 (2005)

V.I. Abramenko, V. Carbone, V. Yurchyshyn, P.R. Goode, R.F. Stein, F. Lepreti, V. Capparelli, A. Vecchio, Turbulent diffusion in the photosphere as derived from photospheric bright point motion. Astrophys. J. **743**, 133 (2011)

T. Amari, J.-F. Luciani, J.-J. Aly, Small-scale dynamo magnetism as the driver for heating the solar atmosphere. Nature **522**, 188–191 (2015). doi:10.1038/nature14478

A. Asensio Ramos, Evidence for quasi-isotropic magnetic fields from Hinode quiet-Sun observations. Astrophys. J. **701**, 1032–1043 (2009). doi:10.1088/0004-637X/701/2/1032

A. Asensio Ramos, M.J. Martínez González, Hierarchical analysis of the quiet-Sun magnetism. Astron. Astrophys. **572**, 98 (2014). doi:10.1051/0004-6361/201423860

H. Auffret, R. Muller, Center-to-limb variation of the network bright points in the solar photosphere. Astron. Astrophys. **246**, 264–279 (1991)

P. Barthol, A. Gandorfer, S.K. Solanki, M. Schüssler, B. Chares, W. Curdt, W. Deutsch, A. Feller, D. Germerott, B. Grauf, K. Heerlein, J. Hirzberger, M. Kolleck, R. Meller, R. Müller, T.L. Riethmüller, G. Tomasch, M. Knölker, B.W. Lites, G. Card, D. Elmore, J. Fox, A. Lecinski, P. Nelson, R. Summers, A. Watt, V. Martínez Pillet, J.A. Bonet, W. Schmidt, T. Berkefeld, A.M. Title, V. Domingo, J.L. Gasent Blesa, J.C. del Toro Iniesta, A. López Jiménez, A. Álvarez-Herrero, L. Sabau-Graziati, C. Widani, P. Haberler, K. Härtel, D. Kampf, T. Levin, I. Pérez Grande, A. Sanz-Andrés, E. Schmidt, The Sunrise mission. Sol. Phys. **268**, 1 (2011)

G.K. Batchelor, On the spontaneous magnetic field in a conducting liquid in turbulent motion. Proc. R. Soc. Lond., Ser. A **201**, 405–416 (1950). doi:10.1098/rspa.1950.0069

C. Beck, L.R. Bellot Rubio, R. Schlichenmaier, P. Sütterlin, Magnetic properties of G-band bright points in a sunspot moat. Astron. Astrophys. **472**, 607–622 (2007)

L.R. Bellot Rubio, D. Orozco Suárez, Pervasive linear polarization signals in the quiet Sun. Astrophys. J. **757**, 19 (2012). doi:10.1088/0004-637X/757/1/19

L.R. Bellot Rubio, B. Ruiz Cobo, M. Collados, Structure of plage flux tubes from the inversion of Stokes spectra. I. Spatially averaged Stokes I and V profiles. Astrophys. J. **535**, 489–500 (2000)

L.R. Bellot Rubio, I. Rodríguez Hidalgo, M. Collados, E. Khomenko, B. Ruiz Cobo, Observation of convective collapse and upward-moving shocks in the quiet Sun. Astrophys. J. **560**, 1010–1019 (2001)

S.V. Berdyugina, S.K. Solanki, C. Frutiger, The molecular Zeeman effect and diagnostics of solar and stellar magnetic fields. II. Synthetic Stokes profiles in the Zeeman regime. Astron. Astrophys. **412**, 513 (2003)

T.E. Berger, A.M. Title, On the relation of G-band bright points to the photospheric magnetic field. Astrophys. J. **553**, 449 (2001)

T.E. Berger, C.J. Schrijver, R.A. Shine, T.D. Tarbell, A.M. Title, G. Scharmer, New observations of subarcsecond photospheric bright points. Astrophys. J. **454**, 531 (1995)

T.E. Berger, M.G. Löfdahl, R.S. Shine, A.M. Title, Measurements of solar magnetic element motion from high-resolution filtergrams. Astrophys. J. **495**, 973–983 (1998)

T.E. Berger, L.H.M. Rouppe van der Voort, M.G. Löfdahl, M. Carlsson, A. Fossum, V.H. Hansteen, E. Marthinussen, A. Title, G. Scharmer, Solar magnetic elements at 0.1 arcsec resolution. General appearance and magnetic structure. Astron. Astrophys. **428**, 613–628 (2004)

T.E. Berger, L. Rouppe van der Voort, M. Löfdahl, Contrast analysis of solar faculae and magnetic bright points. Astrophys. J. **661**, 1272–1288 (2007)

T. Berkefeld, W. Schmidt, D. Soltau, A. Bell, H.P. Doerr, B. Feger, R. Friedlein, K. Gerber, F. Heidecke, T. Kentischer, O. von der Lühe, M. Sigwarth, E. Wälde, P. Barthol, W. Deutsch, A. Gandorfer, D. Germerott, B. Grauf, R. Meller, A. Álvarez-Herrero, M. Knölker, V. Martínez Pillet, S.K. Solanki, A.M. Title, The wave-front correction system for the Sunrise balloon-borne solar observatory. Sol. Phys. **268**, 103 (2011)

P.N. Bernasconi, C.U. Keller, H.P. Povel, J.O. Stenflo, Direct measurements of flux tube inclinations in solar plages. Astron. Astrophys. **302**, 533 (1995)

L. Bharti, R. Jain, C. Joshi, S.N.A. Jaaffrey, G-band bright points and photospheric magnetic fields, in *Astronomical Society of the Pacific Conference Series*, ed. by R. Casini, B.W. Lites. Astronomical Society of the Pacific Conference Series, vol. 358 (2006), p. 61

M. Bianda, R. Ramelli, D. Gisler, J.O. Stenflo, Solar cycle variations of the second solar spectrum, in *Solar Polarization 7*, ed. by K.N. Nagendra, J.O. Stenflo, Q. Qu, M. Samooprna. Astronomical Society of the Pacific Conference Series, vol. 489 (2014), p. 167

J. Blanco Rodríguez, F. Kneer, Faculae at the poles of the Sun revisited: Infrared observations. Astron. Astrophys. **509**, 92 (2010)

J. Blanco Rodríguez, O.V. Okunev, K.G. Puschmann, F. Kneer, B. Sánchez-Andrade Nuño, On the properties of faculae at the poles of the Sun. Astron. Astrophys. **474**, 251–259 (2007)

M. Bodnárová, D. Utz, J. Rybák, On dynamics of G-band bright points. Sol. Phys. **289**, 1543–1556 (2014)

J.M. Borrero, P. Kobel, Inferring the magnetic field vector in the quiet Sun. I. Photon noise and selection criteria. Astron. Astrophys. **527**, 29 (2011). doi:10.1051/0004-6361/201015634

J.M. Borrero, P. Kobel, Inferring the magnetic field vector in the quiet Sun. II. Interpreting results from the inversion of Stokes profiles. Astron. Astrophys. **547**, 89 (2012). doi:10.1051/0004-6361/201118238

J.M. Borrero, P. Kobel, Inferring the magnetic field vector in the quiet Sun. III. Disk variation of the Stokes profiles and isotropism of the magnetic field. Astron. Astrophys. **550**, 98 (2013). doi:10.1051/0004-6361/201118239

J.M. Borrero, V. Martínez-Pillet, R. Schlichenmaier, S.K. Solanki, J.A. Bonet, J.C. del Toro Iniesta, W. Schmidt, P. Barthol, A. Gandorfer, V. Domingo, M. Knölker, Supersonic magnetic upflows in granular cells observed with SUNRISE/IMAX. Astrophys. J. **723**, 144–148 (2010). doi:10.1088/2041-8205/723/2/L144

J.M. Borrero, V. Martínez Pillet, W. Schmidt, C. Quintero Noda, J.A. Bonet, J.C. del Toro Iniesta, L.R. Bellot Rubio, Is magnetic reconnection the cause of supersonic upflows in granular cells? Astrophys. J. **768**, 69 (2013). doi:10.1088/0004-637X/768/1/69

A. Brandenburg, Nonlinear small-scale dynamos at low magnetic Prandtl numbers. Astrophys. J. **741**, 92 (2011). doi:10.1088/0004-637X/741/2/92

A. Brandenburg, K. Subramanian, Astrophysical magnetic fields and nonlinear dynamo theory. Phys. Rep. **417**, 1–209 (2005). doi:10.1016/j.physrep.2005.06.005

A. Brandenburg, D. Sokoloff, K. Subramanian, Current status of turbulent dynamo theory. From large-scale to small-scale dynamos. Space Sci. Rev. **169**, 123–157 (2012). doi:10.1007/s11214-012-9909-x

P.N. Brandt, S.K. Solanki, Solar line asymmetries and the magnetic filling factor. Astron. Astrophys. **231**, 221–234 (1990)

J.H.M.J. Bruls, S.K. Solanki, Infrared lines as probes of solar magnetic features. IX. MgI 12 μm diagnostics of solar plage. Astron. Astrophys. **293**, 240–251 (1995)

J.H.M.J. Bruls, S.K. Solanki, Apparent solar radius variations. The influence of magnetic network and plage. Astron. Astrophys. **427**, 735–743 (2004)

E. Buchlin, Intermittent turbulent dynamo at very low and high magnetic Prandtl numbers. Astron. Astrophys. **534**, 9 (2011). doi:10.1051/0004-6361/201117890

D. Bühler, A. Lagg, S.K. Solanki, Quiet Sun magnetic fields observed by Hinode: Support for a local dynamo. Astron. Astrophys. **555**, 33 (2013). doi:10.1051/0004-6361/201321152

D. Bühler, A. Lagg, S.K. Solanki, M. van Noort, Properties of solar plage from a spatially coupled inversion of Hinode SP data. Astron. Astrophys. **576**, 27 (2015)

M. Bünte, S.K. Solanki, O. Steiner, Centre-to-limb variation of the Stokes V asymmetry in solar magnetic flux tubes. Astron. Astrophys. **268**, 736–748 (1993)

P.J. Bushby, S.M. Houghton, Spatially intermittent fields in photospheric magnetoconvection. Mon. Not. R. Astron. Soc. **362**, 313–320 (2005)

R. Cameron, A. Vögler, M. Schüssler, Decay of a simulated mixed-polarity magnetic field in the solar surface layers. Astron. Astrophys. **533**, 86 (2011)

E.S. Carlin, A. Asensio Ramos, Chromospheric diagnosis with Ca II lines: Forward modeling in forward scattering. I. Astrophys. J. **801**, 16 (2015). doi:10.1088/0004-637X/801/1/16

E.S. Carlin, R. Manso Sainz, A. Asensio Ramos, J. Trujillo Bueno, Scattering polarization in the Ca II infrared triplet with velocity gradients. Astrophys. J. **751**, 5 (2012). doi:10.1088/0004-637X/751/1/5

M. Carlsson, R.F. Stein, Å. Nordlund, G.B. Scharmer, Observational manifestations of solar magnetoconvection: Center-to-limb variation. Astrophys. J. Lett. **610**, 137–140 (2004)

F. Cattaneo, S.M. Tobias, On large-scale dynamo action at high magnetic Reynolds number. Astrophys. J. **789**, 70 (2014). doi:10.1088/0004-637X/789/1/70

F. Cavallini, G. Ceppatelli, A. Righini, Asymmetry and shift of three Fe I photospheric lines in solar active regions. Astron. Astrophys. **143**, 116 (1985)

R. Centeno, H. Socas-Navarro, B. Lites, M. Kubo, Z. Frank, R. Shine, T. Tarbell, A. Title, K. Ichimoto, S. Tsuneta, Y. Katsukawa, Y. Suematsu, T. Shimizu, S. Nagata, Emergence of small-scale magnetic loops in the quiet-Sun internetwork. Astrophys. J. **666**, 137–140 (2007). doi:10.1086/521726

P. Charbonneau, Dynamo models of the solar cycle. Living Rev. Sol. Phys. **7**, 3 (2010). doi:10.12942/lrsp-2010-3, http://www.livingreviews.org/lrsp-2010-3

M.C.M. Cheung, H. Isobe, Flux emergence (theory). Living Rev. Sol. Phys. **11**, 3 (2014)

L.P. Chitta, A.A. van Ballegooijen, L. Rouppe van der Voort, E.E. DeLuca, R. Kariyappa, Dynamics of the solar magnetic bright points derived from their horizontal motions. Astrophys. J. **752**, 48 (2012)

M. Collados, R. López, E. Páez, E. Hernández, M. Reyes, A. Calcines, E. Ballesteros, J.J. Díaz, C. Denker, A. Lagg, R. Schlichenmaier, W. Schmidt, S.K. Solanki, K.G. Strassmeier, O. von der Lühe, R. Volkmer, GRIS: The GREGOR Infrared Spectrograph. Astron. Nachr. **333**, 872 (2012). doi:10.1002/asna.201211738

S. Danilovic, A. Gandorfer, A. Lagg, M. Schüssler, S.K. Solanki, A. Vögler, Y. Katsukawa, S. Tsuneta, The intensity contrast of solar granulation: Comparing Hinode SP results with MHD simulations. Astron. Astrophys. **484**, 17 (2008)

S. Danilovic, B. Beeck, A. Pietarila, M. Schüssler, S.K. Solanki, V. Martínez Pillet, J.A. Bonet, J.C. del Toro Iniesta, V. Domingo, P. Barthol, T. Berkefeld, A. Gandorfer, M. Knölker, W. Schmidt, A.M. Title, Transverse component of the magnetic field in the solar photosphere observed by SUNRISE. Astrophys. J. Lett. **723**, 149–153 (2010a). doi:10.1088/2041-8205/723/2/L149

S. Danilovic, M. Schüssler, S.K. Solanki, Probing quiet Sun magnetism using MURaM simulations and Hinode/SP results: Support for a local dynamo. Astron. Astrophys. **513**, 1 (2010b). doi:10.1051/0004-6361/200913379

S. Danilovic, D. Röhrbein, R.H. Cameron, M. Schüssler, On the relation between continuum brightness and magnetic field in solar active regions. Astron. Astrophys. **550**, 118 (2013)

S. Danilovic, R.H. Cameron, S.K. Solanki, Simulated magnetic flows in the solar photosphere. Astron. Astrophys. **574**, 28 (2015). doi:10.1051/0004-6361/201423779

H. Dara-Papamargaritis, S. Koutchmy, Photospheric faculae-III-intensity, and magnetic field mapping of a typical element of the photospheric network. Astron. Astrophys. **125**, 280–286 (1983)

B. De Pontieu, M. Carlsson, R. Stein, L. Rouppe van der Voort, M. Löfdahl, M. van Noort, Å. Nordlund, G. Scharmer, Rapid temporal variability of faculae: High-resolution observations and modeling. Astrophys. J. **646**, 1405–1420 (2006)

A.G. de Wijn, B.W. Lites, T.E. Berger, Z.A. Frank, T.D. Tarbell, R. Ishikawa, Hinode observations of magnetic elements in internetwork areas. Astrophys. J. **684**, 1469–1476 (2008). doi:10.1086/590237

A.G. de Wijn, J.O. Stenflo, S.K. Solanki, S. Tsuneta, Small-scale solar magnetic fields. Space Sci. Rev. **144**, 275 (2009)

R.J. Defouw, Wave propagation along a magnetic tube. Astrophys. J. **209**, 266–269 (1976)

D. Degenhardt, S.K. Solanki, B. Montesinos, J.H. Thomas, Evidence for siphon flows with shocks in solar magnetic flux tubes. Astron. Astrophys. **279**, 29–32 (1993)

W. Deinzer, G. Hensler, M. Schüssler, E. Weisshaar, Model calculations of magnetic flux tubes. II. Stationary results for solar magnetic elements. Astron. Astrophys. **139**, 435 (1984)

H.W. Dodson, High latitude sunspot, August 13, 1953. Publ. Astron. Soc. Pac. **65**, 256 (1953)

V. Domingo, A. Ortiz, B. Sanahuja, I. Cabello, Centre-to-limb variation of photospheric facular radiance and image resolution. Adv. Space Res. **35**, 345–349 (2005)

V. Domingo, I. Ermolli, P. Fox, C. Fröhlich, M. Haberreiter, N. Krivova, G. Kopp, W. Schmutz, S.K. Solanki, H.C. Spruit, Y. Unruh, A. Vögler, Solar surface magnetism and irradiance on time scales from days to the 11-year cycle. Space Sci. Rev. **145**, 337–380 (2009)

I. Ermolli, K. Matthes, T. Dudok de Wit, N.A. Krivova, K. Tourpali, M. Weber, Y.C. Unruh, L. Gray, U. Langematz, P. Pilewskie, E. Rozanov, W. Schmutz, A. Shapiro, S.K. Solanki, T.N. Woods, Recent variability of the solar spectral irradiance and its impact on climate modelling. Atmos. Chem. Phys. **13**, 3945–3977 (2013)

S. Feng, L. Deng, Y. Yang, K. Ji, Statistical study of photospheric bright points in an active region and quiet Sun. Astrophys. Space Sci. **348**, 17–24 (2013)

A. Ferriz-Mas, M. Schüssler, Waves and instabilities of a toroidal magnetic flux tube in a rotating star. Astrophys. J. **433**, 852–866 (1994)

A. Ferriz-Mas, M. Schüssler, V. Anton, Dynamics of magnetic flux concentrations—the second-order thin flux tube approximation. Astron. Astrophys. **210**, 425–432 (1989)

C.E. Fischer, A.G. de Wijn, R. Centeno, B.W. Lites, C.U. Keller, Statistics of convective collapse events in the photosphere and chromosphere observed with the Hinode SOT. Astron. Astrophys. **504**, 583 (2009)

P. Foukal, P. Bernasconi, H. Eaton, D. Rust, Broadband measurements of facular photometric contrast using the solar bolometric imager. Astrophys. J. Lett. **611**, 57–60 (2004)

C. Frutiger, S.K. Solanki, Empirical models of solar magnetic flux-tubes and their non-magnetic surroundings. Astron. Astrophys. **369**, 646–659 (2001)

A. Gandorfer, B. Grauf, P. Barthol, T.L. Riethmüller, S.K. Solanki, B. Chares, W. Deutsch, S. Ebert, A. Feller, D. Germerott, K. Heerlein, J. Heinrichs, D. Hirche, J. Hirzberger, M. Kolleck, R. Meller, R. Müller, R. Schäfer, G. Tomasch, M. Knölker, V. Martínez Pillet, J.A. Bonet, W. Schmidt, T. Berkefeld, B. Feger, F. Heidecke, D. Soltau, A. Tischenberg, A. Fischer, A. Title, H. Anwand, E. Schmidt, The filter imager SuFI and the Image Stabilization and Light Distribution system ISLiD of the Sunrise balloon-borne observatory: Instrument description. Sol. Phys. **268**, 35 (2011)

M. Gošić, L.R. Bellot Rubio, D. Orozco Suárez, Y. Katsukawa, J.C. del Toro Iniesta, The solar internetwork. I. Contribution to the network magnetic flux. Astrophys. J. **797**, 49 (2014)

D.O. Gough, R.J. Tayler, The influence of a magnetic field on Schwarzschild's criterion for convective instability in an ideally conducting fluid. Mon. Not. R. Astron. Soc. **133**, 85 (1966)

L.J. Gray, J. Beer, M. Geller, J.D. Haigh, M. Lockwood, K. Matthes, U. Cubasch, D. Fleitmann, G. Harrison, L. Hood, J. Luterbacher, G.A. Meehl, D. Shindell, B. van Geel, W. White, Solar influences on climate. Rev. Geophys. **48**, 4001 (2010)

U. Grossmann-Doerth, M. Schüssler, S.K. Solanki, Unshifted, asymmetric Stokes V-profiles—possible solution of a riddle. Astron. Astrophys. **206**, 37–39 (1988)

U. Grossmann-Doerth, M. Knoelker, M. Schüssler, S.K. Solanki, The deep layers of solar magnetic elements. Astron. Astrophys. **285**, 648–654 (1994)

U. Grossmann-Doerth, C.U. Keller, M. Schüssler, Observations of the quiet Sun's magnetic field. Astron. Astrophys. **315**, 610–617 (1996)

U. Grossmann-Doerth, M. Schüssler, O. Steiner, Convective intensification of solar surface magnetic fields: Results of numerical experiments. Astron. Astrophys. **337**, 928–939 (1998)

H.J. Hagenaar, Ephemeral regions on a sequence of full-disk Michelson Doppler imager magnetograms. Astrophys. J. **555**, 448–461 (2001)

H.J. Hagenaar, C.J. Schrijver, A.M. Title, The properties of small magnetic regions on the solar surface and the implications for the solar dynamo(s). Astrophys. J. **584**, 1107–1119 (2003)

G.E. Hale, S.B. Nicholson, The Law of Sun-spot polarity. Astrophys. J. **62**, 270 (1925)

K.L. Harvey, Magnetic bipoles on the Sun, PhD thesis, Univ. Utrecht (1993)

K. Harvey, J. Harvey, Observations of moving magnetic features near sunspots. Sol. Phys. **28**, 61–71 (1973)

K.L. Harvey, S.F. Martin, Ephemeral active regions. Sol. Phys. **32**, 389–402 (1973)

K.L. Harvey, C. Zwaan, Properties and emergence of bipolar active regions. Sol. Phys. **148**, 85–118 (1993)

J.W. Harvey, D. Branston, C.J. Henney, C.U. Keller (SOLIS and GONG Teams), Seething horizontal magnetic fields in the quiet solar photosphere. Astrophys. J. Lett. **659**, 177–180 (2007). doi:10.1086/518036

S.S. Hasan, Convective instability in a solar flux tube. II—Nonlinear calculations with horizontal radiative heat transport and finite viscosity. Astron. Astrophys. **143**, 39–45 (1985)

R.L. Hewitt, S. Shelyag, M. Mathioudakis, F.P. Keenan, Plasma properties and Stokes profiles during the lifetime of a photospheric magnetic bright point. Astron. Astrophys. **565**, 84 (2014)

J. Hirzberger, E. Wiehr, Solar limb faculae. Astron. Astrophys. **438**, 1059–1065 (2005)

J. Hirzberger, A. Feller, T.L. Riethmüller, M. Schüssler, J.M. Borrero, N. Afram, Y.C. Unruh, S.V. Berdyugina, A. Gandorfer, S.K. Solanki, P. Barthol, J.A. Bonet, V. Martínez Pillet, T. Berkefeld, M. Knölker, W. Schmidt, A.M. Title, Quiet-Sun intensity contrasts in the near-ultraviolet as measured from Sunrise. Astrophys. J. Lett. **723**, 154 (2010)

R. Holzreuter, S.K. Solanki, Three-dimensional non-LTE radiative transfer effects in Fe I lines. I. Flux sheet and flux tube geometries. Astron. Astrophys. **547**, 46 (2012)

H. Hotta, M. Rempel, T. Yokoyama, Efficient small-scale dynamo in the solar convection zone. Astrophys. J. **803**, 42 (2015). doi:10.1088/0004-637X/803/1/42

Y. Iida, H.J. Hagenaar, T. Yokoyama, Detection of flux emergence, splitting, merging, and cancellation of network field. I. Splitting and merging. Astrophys. J. **752**, 149 (2012)

R. Ishikawa, S. Tsuneta, Comparison of transient horizontal magnetic fields in a plage region and in the quiet Sun. Astron. Astrophys. **495**, 607–612 (2009). doi:10.1051/0004-6361:200810636

R. Ishikawa, S. Tsuneta, The relationship between vertical and horizontal magnetic fields in the quiet Sun. Astrophys. J. **735**, 74 (2011). doi:10.1088/0004-637X/735/2/74

R. Ishikawa, S. Tsuneta, Y. Kitakoshi, Y. Katsukawa, J.A. Bonet, S. Vargas Domínguez, L.H.M. Rouppe van der Voort, Y. Sakamoto, T. Ebisuzaki, Relationships between magnetic foot points and G-band bright structures. Astron. Astrophys. **472**, 911–918 (2007)

R. Ishikawa, S. Tsuneta, K. Ichimoto, H. Isobe, Y. Katsukawa, B.W. Lites, S. Nagata, T. Shimizu, R.A. Shine, Y. Suematsu, T.D. Tarbell, A.M. Title, Transient horizontal magnetic fields in solar plage regions. Astron. Astrophys. **481**, 25–28 (2008). doi:10.1051/0004-6361:20079022

R. Ishikawa, S. Tsuneta, J. Jurčák, Three-dimensional view of transient horizontal magnetic fields in the photosphere. Astrophys. J. **713**, 1310–1321 (2010). doi:10.1088/0004-637X/713/2/1310

S. Jafarzadeh, S.K. Solanki, A. Lagg, L.R. Bellot Rubio, M. van Noort, A. Feller, S. Danilovic, Inclinations of small quiet-Sun magnetic features based on a new geometric approach. Astron. Astrophys. **569**, 105 (2014a). doi:10.1051/0004-6361/201423414

S. Jafarzadeh, R.H. Cameron, S.K. Solanki, A. Pietarila, A. Feller, A. Lagg, A. Gandorfer, Migration of Ca II H bright points in the internetwork. Astron. Astrophys. **563**, 101 (2014b)

C. Jin, J. Wang, Does the variation of solar inter-network horizontal field follow sunspot cycle? ArXiv e-prints (2015a)

C. Jin, J. Wang, Solar cycle variation of the inter-network magnetic field. Astrophys. J. **806**, 174 (2015b). doi: 10.1088/0004-637X/806/2/174

C.L. Jin, J.X. Wang, Q. Song, H. Zhao, The Sun's small-scale magnetic elements in Solar Cycle 23. Astrophys. J. **731**, 37 (2011)

A.J. Kaithakkal, Y. Suematsu, M. Kubo, D. Shiota, S. Tsuneta, The association of polar faculae with polar magnetic patches examined with Hinode observations. Astrophys. J. **776**, 122 (2013)

A.P. Kazantsev, Enhancement of a magnetic field by a conducting fluid. Sov. Phys. JETP **26**, 1031 (1968)

C.U. Keller, J.O. Stenflo, S.K. Solanki, T.D. Tarbell, A.M. Title, Solar magnetic field strength determinations from high spatial resolution filtergrams. Astron. Astrophys. **236**, 250–255 (1990)

C.U. Keller, M. Schüssler, A. Vögler, V. Zakharov, On the origin of solar faculae. Astrophys. J. Lett. **607**, 59–62 (2004)

E.V. Khomenko, M. Collados, S.K. Solanki, A. Lagg, J. Trujillo Bueno, Quiet-Sun inter-network magnetic fields observed in the infrared. Astron. Astrophys. **408**, 1115–1135 (2003)

L. Kleint, S.V. Berdyugina, A.I. Shapiro, M. Bianda, Solar turbulent magnetic fields: Surprisingly homogeneous distribution during the solar minimum. Astron. Astrophys. **524**, 37 (2010). doi:10.1051/0004-6361/201015285

M. Knoelker, M. Schüssler, Model calculations of magnetic flux tubes. IV—Convective energy transport and the nature of intermediate size flux concentrations. Astron. Astrophys. **202**, 275–283 (1988)

P. Kobel, J. Hirzberger, S.K. Solanki, A. Gandorfer, V. Zakharov, Discriminant analysis of solar bright points and faculae. I. Classification method and center-to-limb distribution. Astron. Astrophys. **502**, 303–314 (2009)

P. Kobel, S.K. Solanki, J.M. Borrero, The continuum contrast of magnetic elements as a function of magnetic field (disk center): Early studies and Hinode/sp results, in *Solar Polarization 6*, ed. by J.R. Kuhn, D.M. Harrington, H. Lin, S.V. Berdyugina, J. Trujillo-Bueno, S.L. Keil, T. Rimmele. Astronomical Society of the Pacific Conference Series, vol. 437 (2011), p. 297

P. Kobel, J. Hirzberger, S.K. Solanki, Discriminant analysis of solar bright points and faculae II. Contrast and morphology analysis. ArXiv e-prints (2014)

R. Kostik, E.V. Khomenko, Properties of convective motions in facular regions. Astron. Astrophys. **545**, 22 (2012)

Ø. Langangen, M. Carlsson, L. Rouppe van der Voort, R.F. Stein, Velocities measured in small-scale solar magnetic elements. Astrophys. J. **655**, 615–623 (2007)

K. Langhans, W. Schmidt, T. Rimmele, Diagnostic spectroscopy of G-band brightenings in the photosphere of the sun. Astron. Astrophys. **423**, 1147–1157 (2004)

J.K. Lawrence, K.P. Topka, H.P. Jones, Contrast of faculae near the disk center and solar variability. J. Geophys. Res. **98**, 18911 (1993)

R.B. Leighton, Observations of solar magnetic fields in plage regions. Astrophys. J. **130**, 366 (1959)

B.W. Lites, A. Skumanich, V. Martinez Pillet, Vector magnetic fields of emerging solar flux. I. Properties at the site of emergence. Astron. Astrophys. **333**, 1053–1068 (1998)

B.W. Lites, G.B. Scharmer, T.E. Berger, A.M. Title, Three-dimensional structure of the active region photosphere as revealed by high angular resolution. Sol. Phys. **221**, 65–84 (2004)

B.W. Lites, M. Kubo, H. Socas-Navarro, T. Berger, Z. Frank, R. Shine, T. Tarbell, A. Title, K. Ichimoto, Y. Katsukawa, S. Tsuneta, Y. Suematsu, T. Shimizu, S. Nagata, The horizontal magnetic flux of the quiet-sun internetwork as observed with the Hinode spectro-polarimeter. Astrophys. J. **672**, 1237–1253 (2008). doi:10.1086/522922

B.W. Lites, R. Centeno, S.W. McIntosh, The solar cycle dependence of the weak internetwork flux. Publ. Astron. Soc. Jpn. **66**, 4 (2014). doi:10.1093/pasj/psu082

W.C. Livingston, Magnetic fields, convection and solar luminosity variability. Nature **297**, 208 (1982)

R. Manso Sainz, M.J. Martínez González, A. Asensio Ramos, Advection and dispersal of small magnetic elements in the very quiet Sun. Astron. Astrophys. **531**, 9 (2011). doi:10.1051/0004-6361/201117042

M.J. Martínez González, L.R. Bellot Rubio, Emergence of small-scale magnetic loops through the quiet solar atmosphere. Astrophys. J. **700**, 1391–1403 (2009). doi:10.1088/0004-637X/700/2/1391

M.J. Martínez González, A. Asensio Ramos, A. López Ariste, R. Manso Sainz, Near-IR internetwork spectropolarimetry at different heliocentric angles. Astron. Astrophys. **479**, 229–234 (2008). doi:10.1051/0004-6361/20078500

M.J. Martínez González, R. Manso Sainz, A. Asensio Ramos, L.R. Bellot Rubio, Small magnetic loops connecting the quiet surface and the hot outer atmosphere of the Sun. Astrophys. J. **714**, 94–97 (2010). doi:10.1088/2041-8205/714/1/L94

M.J. Martínez González, A. Asensio Ramos, R. Manso Sainz, E. Khomenko, V. Martínez Pillet, S.K. Solanki, A. López Ariste, W. Schmidt, P. Barthol, A. Gandorfer, Unnoticed magnetic field oscillations in the very quiet Sun revealed by SUNRISE/IMaX. Astrophys. J. Lett. **730**, 37 (2011a)

M.J. Martínez González, A. Asensio Ramos, R. Manso Sainz, E. Khomenko, V. Martínez Pillet, S.K. Solanki, A. López Ariste, W. Schmidt, P. Barthol, A. Gandorfer, Unnoticed magnetic field oscillations in the very quiet Sun revealed by SUNRISE/IMaX. Astrophys. J. **730**, 37 (2011b). doi:10.1088/2041-8205/730/2/L37

M.J. Martínez González, R. Manso Sainz, A. Asensio Ramos, E. Hijano, Dead calm areas in the very quiet Sun. Astrophys. J. **755**, 175 (2012a). doi:10.1088/0004-637X/755/2/175

M.J. Martínez González, L.R. Bellot Rubio, S.K. Solanki, V. Martínez Pillet, J.C. Del Toro Iniesta, P. Barthol, W. Schmidt, Resolving the internal magnetic structure of the solar network. Astrophys. J. Lett. **758**, 40 (2012b)

V. Martínez Pillet, Solar surface and atmospheric dynamics. The photosphere. Space Sci. Rev. **178**, 141–162 (2013). doi:10.1007/s11214-013-9967-8

V. Martínez Pillet, B.W. Lites, A. Skumanich, Active region magnetic fields. I. Plage fields. Astrophys. J. **474**, 810–842 (1997)

V. Martínez Pillet, J.C. Del Toro Iniesta, A. Álvarez-Herrero, V. Domingo, J.A. Bonet, L. González Fernández, A. López Jiménez, C. Pastor, J.L. Gasent Blesa, P. Mellado, J. Piqueras, B. Aparicio, M. Balaguer, E. Ballesteros, T. Belenguer, L.R. Bellot Rubio, T. Berkefeld, M. Collados, W. Deutsch, A. Feller, F. Girela, B. Grauf, R.L. Heredero, M. Herranz, J.M. Jerónimo, H. Laguna, R. Meller, M. Menéndez, R. Morales, D. Orozco Suárez, G. Ramos, M. Reina, J.L. Ramos, P. Rodríguez, A. Sánchez, N. Uribe-Patarroyo, P. Barthol, A. Gandorfer, M. Knölker, W. Schmidt, S.K. Solanki, S. Vargas Domínguez, The Imaging Magnetograph eXperiment (IMaX) for the Sunrise balloon-borne solar observatory. Sol. Phys. **268**, 57 (2011)

M. Meneguzzi, U. Frisch, A. Pouquet, Helical and nonhelical turbulent dynamos. Phys. Rev. Lett. **47**, 1060–1064 (1981). doi:10.1103/PhysRevLett.47.1060

N. Meunier, J. Zhao, Observations of photospheric dynamics and magnetic fields: From large-scale to small-scale flows. Space Sci. Rev. **144**, 127–149 (2009)

F. Meyer, H.U. Schmidt, Magnetically aligned flows in the solar atmosphere. Astron. J. Suppl. **73**, 71 (1968a)

F. Meyer, H.U. Schmidt, Magnetisch ausgerichtete Strömungen in der Sonnenflecken. Z. Angew. Math. Mech. **48**, 218–221 (1968b)

M.S. Miesch, W.H. Matthaeus, A. Brandenburg, A. Petrosyan, A. Pouquet, C. Cambon, F. Jenko, D. Uzdensky, J. Stone, S. Tobias, J. Toomre, M. Velli, Large-eddy simulations of magnetohydrodynamic turbulence in astrophysics and space physics. ArXiv e-prints (2015)

T. Moran, D. Deming, D.E. Jennings, G. McCabe, Solar magnetic field studies using the 12 micron emission lines. III. Simultaneous measurements at 12 and 1.6 microns. Astrophys. J. **533**, 1035–1042 (2000)

R. Muller, B. Mena, Motions around a decaying sunspot. Sol. Phys. **112**, 295–303 (1987)

R. Muller, T. Roudier, Variability of the quiet photospheric network. Sol. Phys. **94**, 33–47 (1984)

R. Muller, T. Roudier, Latitude and cycle variations of the photospheric network. Sol. Phys. **152**, 131–137 (1994)

S. Nagata, S. Tsuneta, Y. Suematsu, K. Ichimoto, Y. Katsukawa, T. Shimizu, T. Yokoyama, T.D. Tarbell, B.W. Lites, R.A. Shine, T.E. Berger, A.M. Title, L.R. Bellot Rubio, D. Orozco Suárez, Formation of solar magnetic flux tubes with kilogauss field strength induced by convective instability. Astrophys. J. Lett. **677**, 145–147 (2008)

G. Narayan, Transient downflows associated with the intensification of small-scale magnetic features and bright point formation. Astron. Astrophys. **529**, 79 (2011)

G. Narayan, G.B. Scharmer, Small-scale convection signatures associated with a strong plage solar magnetic field. Astron. Astrophys. **524**, 3 (2010)

P. Nisenson, A.A. van Ballegooijen, A.G. de Wijn, P. Sütterlin, Motions of isolated G-band bright points in the solar photosphere. Astrophys. J. **587**, 458–463 (2003)

Å. Nordlund, R.F. Stein, M. Asplund, Solar surface convection. Living Rev. Sol. Phys. **6**, 3 (2009). doi:10.12942/lrsp-2009-2, http://www.livingreviews.org/lrsp-2009-2

D. Orozco Suárez, Y. Katsukawa, On the distribution of quiet-sun magnetic fields at different heliocentric angles. Astrophys. J. **746**, 182 (2012). doi:10.1088/0004-637X/746/2/182

D. Orozco Suárez, L.R. Bellot Rubio, J.C. del Toro Iniesta, S. Tsuneta, B.W. Lites, K. Ichimoto, Y. Katsukawa, S. Nagata, T. Shimizu, R.A. Shine, Y. Suematsu, T.D. Tarbell, A.M. Title, Quiet-Sun internetwork magnetic fields from the inversion of Hinode measurements. Astrophys. J. **670**, 61–64 (2007). doi:10.1086/524139

D. Orozco Suárez, L.R. Bellot Rubio, J.C. del Toro Iniesta, S. Tsuneta, Magnetic field emergence in quiet Sun granules. Astron. Astrophys. **481**, 33 (2008)

D. Orozco Suárez, Y. Katsukawa, L.R. Bellot Rubio, The connection between internetwork magnetic elements and supergranular flows. Astrophys. J. **758**, 38 (2012). doi:10.1088/2041-8205/758/2/L38

A. Ortiz, S.K. Solanki, V. Domingo, M. Fligge, B. Sanahuja, On the intensity contrast of solar photospheric faculae and network elements. Astron. Astrophys. **388**, 1036–1047 (2002)

A. Ortiz, V. Domingo, B. Sanahuja, The intensity contrast of solar photospheric faculae and network elements. II. Evolution over the rising phase of solar cycle 23. Astron. Astrophys. **452**, 311–319 (2006)

E.N. Parker, The formation of sunspots from the solar toroidal field. Astrophys. J. **121**, 491 (1955)

E.N. Parker, Topological dissipation and the small-scale fields in turbulent gases. Astrophys. J. **174**, 499 (1972). doi:10.1086/151512

E.N. Parker, The reconnection rate of magnetic fields. Astrophys. J. **180**, 247–252 (1973). doi:10.1086/151959

E.N. Parker, Hydraulic concentration of magnetic fields in the solar photosphere. VI—Adiabatic cooling and concentration in downdrafts. Astrophys. J. **221**, 368–377 (1978)

C.E. Parnell, C.E. DeForest, H.J. Hagenaar, B.A. Johnston, D.A. Lamb, B.T. Welsch, A power-law distribution of solar magnetic fields over more than five decades in flux. Astrophys. J. **698**, 75–82 (2009)

V. Penza, B. Caccin, I. Ermolli, M. Centrone, Comparison of model calculations and photometric observations of bright "magnetic" regions. Astron. Astrophys. **413**, 1115–1123 (2004)

K. Petrovay, G. Szakaly, The origin of intranetwork fields: A small-scale solar dynamo. Astron. Astrophys. **274**, 543 (1993)

K. Petrovay, V. Martínez Pillet, L. van Driel-Gesztelyi, Making sense of sunspot decay—II. Deviations from the mean law and plage effects. Sol. Phys. **188**, 315–330 (1999)

J. Pietarila Graham, S. Danilovic, M. Schüssler, Turbulent magnetic fields in the quiet Sun: Implications of Hinode observations and small-scale dynamo simulations. Astrophys. J. **693**, 1728–1735 (2009). doi:10.1088/0004-637X/693/2/1728

J. Pietarila Graham, R. Cameron, M. Schüssler, Turbulent small-scale dynamo action in solar surface simulations. Astrophys. J. **714**, 1606–1616 (2010). doi:10.1088/0004-637X/714/2/1606

A. Pietarila, R. Cameron, S.K. Solanki, Expansion of magnetic flux concentrations: A comparison of Hinode SOT data and models. Astron. Astrophys. **518**, 50 (2010)

A. Pietarila, R.H. Cameron, S. Danilovic, S.K. Solanki, Transport of magnetic flux from the canopy to the internetwork. Astrophys. J. **729**, 136 (2011). doi:10.1088/0004-637X/729/2/136

G.W. Pneuman, S.K. Solanki, J.O. Stenflo, Structure and merging of solar magnetic fluxtubes. Astron. Astrophys. **154**, 231–242 (1986)

C. Quintero Noda, V. Martínez Pillet, J.M. Borrero, S.K. Solanki, Temporal relation between quiet-Sun transverse fields and the strong flows detected by IMaX/SUNRISE. Astron. Astrophys. **558**, 30 (2013). doi:10.1051/0004-6361/201321719

C. Quintero Noda, J.M. Borrero, D. Orozco Suárez, B. Ruiz Cobo, High speed magnetized flows in the quiet Sun. Astron. Astrophys. **569**, 73 (2014). doi:10.1051/0004-6361/201424131

C. Quintero Noda, B. Ruiz Cobo, D. Orozco Suárez, Photospheric downward plasma motions in the quiet Sun. Astron. Astrophys. **566**, 139 (2014). doi:10.1051/0004-6361/201423461

D. Rabin, A true-field magnetogram in a solar plage region. Astrophys. J. Lett. **390**, 103–106 (1992a)

D. Rabin, Spatially extended measurements of magnetic field strength in solar plages. Astrophys. J. **391**, 832–844 (1992b)

M. Rempel, Numerical simulations of quiet Sun magnetism: On the contribution from a small-scale dynamo. Astrophys. J. **789**, 132 (2014). doi:10.1088/0004-637X/789/2/132

M. Rempel, R. Schlichenmaier, Sunspot modeling: From simplified models to radiative MHD simulations. Living Rev. Sol. Phys. **8**, 3 (2011). doi:10.12942/lrsp-2011-3, http://www.livingreviews.org/lrsp-2011-3

M. Rempel, M. Schüssler, M. Knölker, Radiative magnetohydrodynamic simulation of sunspot structure. Astrophys. J. **691**, 640–649 (2009). doi:10.1088/0004-637X/691/1/640

I.S. Requerey, J.C. Del Toro Iniesta, L.R. Bellot Rubio, J.A. Bonet, V. Martínez Pillet, S.K. Solanki, W. Schmidt, The history of a quiet-sun magnetic element revealed by IMaX/SUNRISE. Astrophys. J. **789**, 6 (2014)

R. Rezaei, O. Steiner, S. Wedemeyer-Böhm, R. Schlichenmaier, W. Schmidt, B.W. Lites, Hinode observations reveal boundary layers of magnetic elements in the solar photosphere. Astron. Astrophys. **476**, 33–36 (2007)

T.L. Riethmüller, S.K. Solanki, V. Martínez Pillet, J. Hirzberger, A. Feller, J.A. Bonet, N. Bello González, M. Franz, M. Schüssler, P. Barthol, T. Berkefeld, J.C. del Toro Iniesta, V. Domingo, A. Gandorfer, M. Knölker, W. Schmidt, Bright points in the quiet Sun as observed in the visible and near-UV by the balloon-borne observatory SUNRISE. Astrophys. J. Lett. **723**, 169–174 (2010)

T.L. Riethmüller, S.K. Solanki, S.V. Berdyugina, M. Schüssler, V. Martínez Pillet, A. Feller, A. Gandorfer, J. Hirzberger, Comparison of solar photospheric bright points between Sunrise observations and MHD simulations. Astron. Astrophys. **568**, 13 (2014)

D. Röhrbein, R. Cameron, M. Schüssler, Is there a non-monotonic relation between photospheric brightness and magnetic field strength in solar plage regions? Astron. Astrophys. **532**, 140 (2011)

P. Romano, F. Berrilli, S. Criscuoli, D. Del Moro, I. Ermolli, F. Giorgi, B. Viticchié, F. Zuccarello, A comparative analysis of photospheric bright points in an active region and in the quiet Sun. Sol. Phys. **280**, 407–416 (2012)

L.H.M. Rouppe van der Voort, V.H. Hansteen, M. Carlsson, A. Fossum, E. Marthinussen, M.J. van Noort, T.E. Berger, Solar magnetic elements at 0.1 arcsec resolution. II. Dynamical evolution. Astron. Astrophys. **435**, 327–337 (2005)

F. Rubio da Costa, S.K. Solanki, S. Danilovic, J. Hizberger, V. Martínez-Pillet, Centre-to-limb properties of small, photospheric quiet-Sun jets. Astron. Astrophys. **574**, 95 (2015). doi:10.1051/0004-6361/201424880

I. Rüedi, S.K. Solanki, D. Rabin, Infrared lines as probes of solar magnetic features. IV—Discovery of a siphon flow. Astron. Astrophys. **261**, 21–24 (1992a)

I. Rüedi, S.K. Solanki, W. Livingston, J.O. Stenflo, Infrared lines as probes of solar magnetic features. III—Strong and weak magnetic fields in plages. Astron. Astrophys. **263**, 323–338 (1992b)

R.J. Rutten, D. Kiselman, L. Rouppe van der Voort, B. Plez, Proxy magnetometry of the photosphere: Why are G-band bright points so bright?, in *Advanced Solar Polarimetry—Theory, Observation, and Instrumentation*, ed. by M. Sigwarth. Astronomical Society of the Pacific Conference Series, vol. 236 (2001), p. 445

A. Sainz Dalda, J. Martínez-Sykora, L. Bellot Rubio, A. Title, Study of single-lobed circular polarization profiles in the quiet Sun. Astrophys. J. **748**, 38 (2012). doi:10.1088/0004-637X/748/1/38

J. Sánchez Almeida, Inter-Network magnetic fields observed during the minimum of the solar cycle. Astron. Astrophys. **411**, 615–621 (2003). doi:10.1051/0004-6361:20031560

J. Sánchez Almeida, B.W. Lites, Physical properties of the solar magnetic photosphere under the MISMA hypothesis. II. Network and internetwork fields at the disk center. Astrophys. J. **532**, 1215–1229 (2000)

J. Sanchez Almeida, V. Martinez Pillet, The inclination of network magnetic fields. Astrophys. J. **424**, 1014 (1994)

J. Sánchez Almeida, A. Asensio Ramos, J. Trujillo Bueno, J. Cernicharo, G-band spectral synthesis in solar magnetic concentrations. Astrophys. J. **555**, 978–989 (2001)

J. Sánchez Almeida, J.A. Bonet, B. Viticchié, D. Del Moro, Magnetic bright points in the quiet Sun. Astrophys. J. Lett. **715**, 26–29 (2010). doi:10.1088/2041-8205/715/1/L26

G.B. Scharmer, K. Bjelksjo, T.K. Korhonen, B. Lindberg, B. Petterson, The 1-meter Swedish Solar Telescope, in *Society of Photo-Optical Instrumentation Engineers (SPIE) Conference Series*, ed. by S.L. Keil, S.V. Avakyan. SPIE Conf. Ser., vol. 4853 (2003), p. 341

G.B. Scharmer, J. de la Cruz Rodriguez, P. Sütterlin, V.M.J. Henriques, Opposite polarity field with convective downflow and its relation to magnetic spines in a sunspot penumbra. Astron. Astrophys. **553**, 63 (2013)

R.S. Schnerr, H.C. Spruit, The brightness of magnetic field concentrations in the quiet Sun. Astron. Astrophys. **532**, 136 (2011)

C.J. Schrijver, C. Zwaan, *Solar and Stellar Magnetic Activity* (Cambridge University Press, New York, 2000)

C.J. Schrijver, A.M. Title, A.A. van Ballegooijen, H.J. Hagenaar, R.A. Shine, Sustaining the quiet photospheric network: The balance of flux emergence, fragmentation, merging, and cancellation. Astrophys. J. **487**, 424–436 (1997)

C.J. Schrijver, A.M. Title, K.L. Harvey, N.R. Sheeley, Y.-M. Wang, G.H.J. van den Oord, R.A. Shine, T.D. Tarbell, N.E. Hurlburt, Large-scale coronal heating by the small-scale magnetic field of the Sun. Nature **394**, 152–154 (1998)

M. Schüssler, MHD models of solar photospheric magnetic flux concentrations, in *Small Scale Magnetic Flux Concentrations in the Solar Photosphere*, ed. by W. Deinzer, M. Knölker, H.H. Voigt (1986), p. 103

M. Schüssler, Theoretical aspects of small-scale photospheric magnetic fields, in *Solar Photosphere: Structure, Convection and Magnetic Fields*, ed. by J.O. Stenflo. IAU Symposium, vol. 138 (Kluwer/Springer, Dordrecht, 1990), p. 161

M. Schüssler, Solar Magneto-convection, in *Solar and astrophysical dynamos and magnetic activity*, ed. by A.G. Kosovichev, E. de Gouveia Dal Pino, Y. Yan. IAU Symposium, vol. 294 (Cambridge University Press, Cambridge, 2013), pp. 95–106. doi:10.1017/S1743921313002329

M. Schüssler, S.K. Solanki, Continuum intensity of magnetic flux concentrations—are magnetic elements bright points? Astron. Astrophys. **192**, 338–342 (1988)

M. Schüssler, A. Vögler, Strong horizontal photospheric magnetic field in a surface dynamo simulation. Astron. Astrophys. **481**, 5–8 (2008). doi:10.1051/0004-6361:20078998

M. Schüssler, S. Shelyag, S. Berdyugina, A. Vögler, S.K. Solanki, Why solar magnetic flux concentrations are bright in molecular bands. Astrophys. J. Lett. **597**, 173–176 (2003)

N. Shchukina, J. Trujillo Bueno, Determining the magnetization of the quiet Sun photosphere from the Hanle effect and surface dynamo simulations. Astrophys. J. Lett. **731**, 21 (2011). doi:10.1088/2041-8205/731/1/L21

S. Shelyag, M. Schüssler, S.K. Solanki, S.V. Berdyugina, A. Vögler, G-band spectral synthesis and diagnostics of simulated solar magneto-convection. Astron. Astrophys. **427**, 335–343 (2004)

S. Shelyag, M. Schüssler, S.K. Solanki, A. Vögler, Stokes diagnostics of simulated solar magneto-convection. Astron. Astrophys. **469**, 731–747 (2007)

T. Shimizu, B.W. Lites, Y. Katsukawa, K. Ichimoto, Y. Suematsu, S. Tsuneta, S. Nagata, M. Kubo, R.A. Shine, T.D. Tarbell, Frequent occurrence of high-speed local mass downflows on the solar surface. Astrophys. J. **680**, 1467–1476 (2008)

M. Sigwarth, Properties and origin of asymmetric and unusual Stokes V profiles observed in solar magnetic fields. Astrophys. J. **563**, 1031–1044 (2001)

M. Sigwarth, K.S. Balasubramaniam, M. Knölker, W. Schmidt, Dynamics of solar magnetic elements. Astron. Astrophys. **349**, 941–955 (1999)

S.K. Solanki, Velocities in solar magnetic fluxtubes. Astron. Astrophys. **168**, 311–329 (1986)

S.K. Solanki, The origin and the diagnostic capabilities of the Stokes V asymmetry observed in solar faculae and the network. Astron. Astrophys. **224**, 225–241 (1989)

S.K. Solanki, Smallscale solar magnetic fields—an overview. Space Sci. Rev. **63**, 1–188 (1993)

S.K. Solanki, Sunspots: An overview. Astron. Astrophys. Rev. **11**, 153–286 (2003)

S.K. Solanki, O. Steiner, How magnetic is the solar chromosphere? Astron. Astrophys. **234**, 519 (1990)

S.K. Solanki, J.O. Stenflo, Properties of solar magnetic fluxtubes as revealed by Fe I lines. Astron. Astrophys. **140**, 185–198 (1984)

S.K. Solanki, J.O. Stenflo, Models of solar magnetic fluxtubes—constraints imposed by Fe I and II lines. Astron. Astrophys. **148**, 123–132 (1985)

S.K. Solanki, D. Zufferey, H. Lin, I. Rüedi, J.R. Kuhn, Infrared lines as probes of solar magnetic features. XII. Magnetic flux tubes: evidence of convective collapse? Astron. Astrophys. **310**, 33–36 (1996)

S.K. Solanki, W. Finsterle, I. Rüedi, W. Livingston, Expansion of solar magnetic flux tubes large and small. Astron. Astrophys. **347**, 27 (1999)

S.K. Solanki, B. Inhester, M. Schüssler, The solar magnetic field. Rep. Prog. Phys. **69**, 563–668 (2006)

S.K. Solanki, P. Barthol, S. Danilovic, A. Feller, A. Gandorfer, J. Hirzberger, T.L. Riethmüller, M. Schüssler, J.A. Bonet, V. Martínez Pillet, J.C. del Toro Iniesta, V. Domingo, J. Palacios, M. Knölker, N. Bello González, T. Berkefeld, M. Franz, W. Schmidt, A.M. Title, Sunrise: Instrument, mission, data, and first results. Astrophys. J. Lett. **723**, 127 (2010)

S.K. Solanki, N.A. Krivova, J.D. Haigh, Solar irradiance variability and climate. Annu. Rev. Astron. Astrophys. **51**, 311–351 (2013). doi:10.1146/annurev-astro-082812-141007

H.C. Spruit, Pressure equilibrium and energy balance of small photospheric fluxtubes. Sol. Phys. **50**, 269 (1976)

H.C. Spruit, Magnetic flux tubes and transport of heat in the convection zone of the Sun, PhD thesis, University of Utrecht, The Netherlands (1977)

H.C. Spruit, Convective collapse of flux tubes. Sol. Phys. **61**, 363–378 (1979)

H.C. Spruit, Magnetic flux tubes. NASA Spec. Publ. **450**, 385 (1981)

H.C. Spruit, Theory of photospheric magnetic fields, in *Solar and Stellar Magnetic Fields: Origins and Coronal Effects*, ed. by J.O. Stenflo. IAU Symposium, vol. 102 (1983), p. 41

H.C. Spruit, E.G. Zweibel, Convective instability of thin flux tubes. Sol. Phys. **62**, 15–22 (1979)

J. Squire, A. Bhattacharjee, Generation of large-scale magnetic fields by small-scale dynamo in shear flows. ArXiv e-prints (2015)

S. Stangl, J. Hirzberger, On small scale magnetic structures in the solar photosphere. Astron. Astrophys. **432**, 319–329 (2005)

R.F. Stein, Solar surface magneto-convection. Living Rev. Sol. Phys. **9**, 4 (2012). doi:10.12942/lrsp-2012-4, http://www.livingreviews.org/lrsp-2012-4

O. Steiner, Photospheric magnetic field at small scales, in *Turbulence, Waves, and Instabilities in the Solar Plasma*, ed. by R. Erdelyi, K. Petrovay, B. Roberts, M. Aschwanden. NATO Advanced Research Workshop (2003), p. 117

O. Steiner, Radiative properties of magnetic elements. II. Center to limb variation of the appearance of photospheric faculae. Astron. Astrophys. **430**, 691–700 (2005)

O. Steiner, R. Rezaei, Recent advances in the exploration of the small-scale structure of the quiet Solar atmosphere: Vortex flows, the horizontal magnetic field, and the Stokes-V Line-ratio method, in *Fifth Hinode Science Meeting*, ed. by L. Golub, I. De Moortel, T. Shimizu. Astronomical Society of the Pacific Conference Series, vol. 456 (2012), p. 3

O. Steiner, U. Grossmann-Doerth, M. Schüssler, M. Sigwarth, The formation of extremely asymmetric Stokes V profiles, in *Astronomische Gesellschaft Meeting Abstracts*, ed. by R.E. Schielicke. Astronomische Gesellschaft Meeting Abstracts, vol. 15 (1999), p. 11

O. Steiner, P.H. Hauschildt, J. Bruls, Radiative properties of magnetic elements. I. Why are G-band bright points bright? Astron. Astrophys. **372**, 13 (2001)

O. Steiner, R. Rezaei, W. Schaffenberger, S. Wedemeyer-Böhm, The horizontal internetwork magnetic field: Numerical simulations in comparison to observations with Hinode. Astrophys. J. **680**, 85–88 (2008). doi:10.1086/589740

J.O. Stenflo, Magnetic-field structure of the photospheric network. Sol. Phys. **32**, 41–63 (1973)

J.O. Stenflo, Solar magnetic flux at small scales (invited review), in *Solar Magnetic Fields*, ed. by M. Schüssler, W. Schmidt (1994), p. 301

J.O. Stenflo, Distribution functions for magnetic fields on the quiet Sun. Astron. Astrophys. **517**, 37 (2010). doi:10.1051/0004-6361/200913972

J.O. Stenflo, Collapsed, uncollapsed, and hidden magnetic flux on the quiet Sun. Astron. Astrophys. **529**, 42 (2011)

J.O. Stenflo, Horizontal or vertical magnetic fields on the quiet Sun. Angular distributions and their height variations. Astron. Astrophys. **555**, 132 (2013). doi:10.1051/0004-6361/201321608

J.O. Stenflo, J.W. Harvey, Dependence of the properties of magnetic fluxtubes on area factor or amount of flux. Sol. Phys. **95**, 99–118 (1985)

J.O. Stenflo, S. Solanki, J.W. Harvey, J.W. Brault, Diagnostics of solar magnetic fluxtubes using a Fourier transform spectrometer. Astron. Astrophys. **131**, 333–346 (1984)

J.O. Stenflo, S.K. Solanki, J.W. Harvey, Center-to-limb variation of Stokes profiles and the diagnostics of solar magnetic fluxtubes. Astron. Astrophys. **171**, 305–316 (1987)

L.G. Stenholm, J.O. Stenflo, Multi-dimensional non-LTE radiative transfer in magnetic fluxtubes on the sun. Astron. Astrophys. **58**, 273 (1977)

A. Takeuchi, On the formation of intense solar photospheric flux tubes, in *IAU Joint Discussion*. IAU Joint Discussion, vol. 19 (1997), p. 51

I. Thaler, H.C. Spruit, Small-scale dynamos on the solar surface: Dependence on magnetic Prandtl number. Astron. Astrophys. **578**, 54 (2015). doi:10.1051/0004-6361/201423738

J.H. Thomas, B. Montesinos, Siphon flows in isolated magnetic flux tubes. III—The equilibrium path of the flux-tube arch. Astrophys. J. **359**, 550–559 (1990). doi:10.1086/169086

L.M. Thornton, C.E. Parnell, Small-scale flux emergence observed using Hinode/SOT. Sol. Phys. **269**, 13 (2011)

A.M. Title, T.D. Tarbell, K.P. Topka, S.H. Ferguson, R.A. Shine (SOUP Team), Statistical properties of solar granulation derived from the SOUP instrument on Spacelab 2. Astrophys. J. **336**, 475–494 (1989)

A.M. Title, K.P. Topka, T.D. Tarbell, W. Schmidt, C. Balke, G. Scharmer, On the differences between plage and quiet sun in the solar photosphere. Astrophys. J. **393**, 782–794 (1992)

S.M. Tobias, F. Cattaneo, S. Boldyrev, MHD dynamos and turbulence, in *Ten Chapters in Turbulence*, ed. by P.A. Davidson, Y. Kaneda, K.R. Sreenivasan (Cambridge University Press, Cambridge, 2013), pp. 351–404

K.P. Topka, T.D. Tarbell, A.M. Title, Properties of the smallest solar magnetic elements. I. Facular contrast near sun center. Astrophys. J. **396**, 351–363 (1992)

K.P. Topka, T.D. Tarbell, A.M. Title, Properties of the smallest solar magnetic elements. II. Observations versus hot wall models of faculae. Astrophys. J. **484**, 479–486 (1997)

S. Tsuneta, K. Ichimoto, Y. Katsukawa, S. Nagata, M. Otsubo, T. Shimizu, Y. Suematsu, M. Nakagiri, M. Noguchi, T. Tarbell, A. Title, R. Shine, W. Rosenberg, C. Hoffmann, B. Jurcevich, G. Kushner, M. Levay, B. Lites, D. Elmore, T. Matsushita, N. Kawaguchi, H. Saito, I. Mikami, L.D. Hill, J.K. Owens, The Solar Optical Telescope for the Hinode mission: An overview. Sol. Phys. **249**, 167 (2008)

H. Uitenbroek, A. Tritschler, The contrast of magnetic elements in synthetic CH- and CN-band images of solar magnetoconvection. Astrophys. J. **639**, 525–533 (2006)

H. Uitenbroek, A. Tritschler, Narrow-band imaging in the CN band at 388.33 nm. Astron. Astrophys. **462**, 1157–1163 (2007)

H. Uitenbroek, A. Tritschler, T. Rimmele, The discrepancy in G-band contrast: Where is the quiet Sun? Astrophys. J. **668**, 586–593 (2007)

R.K. Ulrich, L. Bertello, Solar-cycle dependence of the Sun's apparent radius in the neutral iron spectral line at 525 nm. Nature **377**, 214 (1995)

D. Utz, A. Hanslmeier, C. Möstl, R. Muller, A. Veronig, H. Muthsam, The size distribution of magnetic bright points derived from Hinode/SOT observations. Astron. Astrophys. **498**, 289–293 (2009)

D. Utz, A. Hanslmeier, R. Muller, A. Veronig, J. Rybák, H. Muthsam, Dynamics of isolated magnetic bright points derived from Hinode/SOT G-band observations. Astron. Astrophys. **511**, 39 (2010). doi:10.1051/0004-6361/200913085

D. Utz, J. Jurčák, A. Hanslmeier, R. Muller, A. Veronig, O. Kühner, Magnetic field strength distribution of magnetic bright points inferred from filtergrams and spectro-polarimetric data. Astron. Astrophys. **554**, 65 (2013)

D. Utz, J.C. del Toro Iniesta, L.R. Bellot Rubio, J. Jurčák, V. Martínez Pillet, S.K. Solanki, W. Schmidt, The formation and disintegration of magnetic bright points observed by Sunrise/IMaX. Astrophys. J. **796**, 79 (2014)

A.A. van Ballegooijen, P. Nisenson, R.W. Noyes, M.G. Löfdahl, R.F. Stein, Å. Nordlund, V. Krishnakumar, Dynamics of magnetic flux elements in the solar photosphere. Astrophys. J. **509**, 435–447 (1998)

P. Venkatakrishnan, Inhibition of convective collapse of solar magnetic flux tubes by radiative diffusion. Nature **322**, 156 (1986)

B. Viticchié, On the polarimetric signature of emerging magnetic loops in the quiet Sun. Astrophys. J. **747**, 36 (2012). doi:10.1088/2041-8205/747/2/L36

B. Viticchié, D. Del Moro, S. Criscuoli, F. Berrilli, Imaging spectropolarimetry with IBIS. II. On the fine structure of G-band bright features. Astrophys. J. **723**, 787–796 (2010)

B. Viticchié, J. Sánchez Almeida, D. Del Moro, F. Berrilli, Interpretation of HINODE SOT/SP asymmetric Stokes profiles observed in the quiet Sun network and internetwork. Astron. Astrophys. **526**, 60 (2011)

A. Vögler, M. Schüssler, A solar surface dynamo. Astron. Astrophys. **465**, 43–46 (2007). doi:10.1051/0004-6361:20077253

A. Vögler, S. Shelyag, M. Schüssler, F. Cattaneo, T. Emonet, T. Linde, Simulations of magneto-convection in the solar photosphere. Equations, methods, and results of the MURaM code. Astron. Astrophys. **429**, 335–351 (2005)

A.R. Webb, B. Roberts, Vertical motions in an intense magnetic flux tube. II—Convective instability. Sol. Phys. **59**, 249–274 (1978)

T. Wiegelmann, J.K. Thalmann, S.K. Solanki, The magnetic field in the solar atmosphere. Astron. Astrophys. Rev. **22**, 78 (2014)

E. Wiehr, A unique magnetic field range for nonspot solar magnetic regions. Astron. Astrophys. **69**, 279 (1978)

L. Yelles Chaouche, S.K. Solanki, M. Schüssler, Comparison of the thin flux tube approximation with 3D MHD simulations. Astron. Astrophys. **504**, 595 (2009)

K.L. Yeo, S.K. Solanki, N.A. Krivova, Intensity contrast of solar network and faculae. Astron. Astrophys. **550**, 95 (2013)

K.L. Yeo, N.A. Krivova, S.K. Solanki, Solar cycle variation in solar irradiance. Space Sci. Rev. **186**, 137–167 (2014). doi:10.1007/s11214-014-0061-7

V. Zakharov, A. Gandorfer, S.K. Solanki, M. Löfdahl, A comparative study of the contrast of solar magnetic elements in CN and CH. Astron. Astrophys. **437**, 43–46 (2005)

I. Zayer, S.K. Solanki, J.O. Stenflo, The internal magnetic field distribution and the diameters of solar magnetic elements. Astron. Astrophys. **211**, 463–475 (1989)

I. Zayer, J.O. Stenflo, C.U. Keller, S.K. Solanki, Dependence of the properties of solar magnetic flux tubes on filling factor. II—Results of an inversion approach. Astron. Astrophys. **239**, 356–366 (1990)

I.B. Zeldovich, A.A. Ruzmaikin, D.D. Sokolov, *Magnetic Fields in Astrophysics* (Gordon & Breach, New York, 1983)

H. Zhang, M. Song, Vector magnetogram and Dopplergram observation of magnetic flux emergence and its explanation. Sol. Phys. **138**, 69–92 (1992)

G. Zhou, J. Wang, C. Jin, Solar intranetwork magnetic elements: Flux distributions. Sol. Phys. **283**, 273 (2013)

H. Zirin, Weak solar fields and their connection to the solar cycle. Sol. Phys. **110**, 101–107 (1987)

H. Zirin, B. Popp, Observations of the 12 micron MG I lines in various solar features. Astrophys. J. **340**, 571–578 (1989)

C. Zwaan, The emergence of magnetic flux. Sol. Phys. **100**, 397–414 (1985)